J. Fluid Mech. (1983), *vol.* 131, *pp.* 219–249
Printed in Great Britain

Interacting flow theory and trailing edge separation – no stall

By F. T. SMITH†
United Technologies Research Center, East Hartford, Connecticut, U.S.A.

(Received 17 June 1982)

The central question addressed here concerns the occurrence of laminar separation near a non-symmetric trailing edge, on one surface only of an airfoil, and whether or not such an event heralds a 'catastrophic stall' in the sense that the flow structure changes significantly from the triple-deck or interactive-boundary-layer form holding for attached flow. Virtually all previous works have conjectured, assumed or argued that there is such a catastrophic stall. The present work, however, points (strongly, we believe) to the opposite view, based on a combination of analytical and numerical grounds. First, the argument for a catastrophic stall, although tempting, is shown to contain a fundamental flaw. Secondly, the present numerical work deliberately aims at including the most important separated-flow features, the acknowledgement of the discontinuities at the trailing-edge station and the effects of reversed flow, in a systematic fashion. This appears to be the first such attempt. As a result the trailing-edge requirements are found to be swept upstream, forcing any flow reversal on just one surface to be followed by a reattachment, however abruptly, just before the trailing-edge point. Thirdly, an analysis of the nearly separated and the just-separated regimes confirms the natural emergence of the reattachment phenomenon and ties in closely with the observed numerical features. In particular, the distance of the reattachment point from the trailing edge is found to be of the tiny order $\bar{A}^4$ or less, where $\bar{A}$ is the small upstream separation distance. Finally, there is shown to be a logical tie-in also with trailing-edge flows involving two-sided separation where no catastrophic stall arises. It is concluded that there is *no catastrophic stall* and that *inter alia* the triple-deck/interactive-boundary-layer approach can continue to be used with one-sided separation present.

The study implies some fairly striking features associated with one-sided separating flows, but these do bear a firm resemblance to recent laminar and even turbulent flow computations and experiments. This indicates that, contrary to previous proposals, such computations and experiments are explicable within the realms of interactive-boundary-layer theory.

1. Introduction

The part played by the trailing edge of an airfoil in flight is vital. If the main flow past the airfoil departs significantly from the surface shape ahead of the trailing edge, the adverse consequences for the lift and drag can be substantial. With this in mind we address the matter of trailing-edge stall, for a non-symmetric airfoil fixed in an otherwise uniform stream. Theoretically, is there a 'catastrophic stall' (in the

† Permanent address: Mathematics Department, Imperial College, London, SW7 2BZ, U.K.

sense of a breakdown, failure and hence, of most physical importance and danger, a discontinuous change in the entire steady flow structure) when flow departure or separation first occurs ahead of the trailing edge on just one of the airfoil surfaces? This central question arises because of the Rott–Hakkinen condition (Hakkinen & Rott 1965) for high Reynolds number motions where the interactive-boundary-layer equations control events, for most separated or attached motions at least. The condition is that, if the flow is forward on one side of the surface (say the lower side), at the onset of the trailing edge, then it must also be forward there on the other, upper, side. As a result it has been argued, conjectured or assumed in a number of very interesting previous works in this area (see Brown & Stewartson 1970; Stewartson 1974; Messiter 1979; Daniels 1974; Melnik & Chow 1975; Chow & Melnik 1976; Veldman 1980; Brown & Cheng 1981; Stewartson 1981) that, once one-sided separation occurs, there must be such a catastrophic stall or failure because the Rott–Hakkinen forward-flow condition is violated, and so a new flow structure must arise. If so, there could be a drastic effect on the airfoil performance.

This study advances the opposite view, however, based on the analytical and numerical arguments to be described subsequently. Our point is that once separation does occur, say on the upper surface ahead of the trailing edge, then beyond separation the very presence of reversed flow allows upstream transmission of information locally. So, in particular, the information concerning the requirement of forward flow at the trailing edge can be transmitted upstream, thereby forcing the flow upstream to adjust itself in readiness for the Rott–Hakkinen constraint further downstream, in principle. Such an adjustment requires a reattachment to take place between the positions of the separation point and the trailing edge, of course. The analysis and calculations described in this investigation support strongly (we believe) the view that reattachment does indeed occur and that accordingly there is no catastrophic stall or discontinuous change. Hence the effect on airfoil performance is not so drastic.

The governing equations and boundary conditions are introduced in §2. Specifically, we take a thin airfoil whose main non-symmetry is confined to the trailing-edge area within the triple-deck: Stewartson 1969; Messiter 1970; Brown & Stewartson 1970), other less local non-symmetries being of secondary importance at this stage. Either the usual triple-deck or a condensed problem, concerning a slightly more abrupt trailing-edge geometry, is suitable for the investigation of the matter of stall. The condensed problem in fact serves to emphasize the role of the reversed flow while losing nothing central to the issue. Finite-difference numerical solutions for these local flows are presented in §3. Three crucial parts of the numerical treatments are: (i) the use of appropriate windward differencing to allow for the upstream transmission of information through the reversed flow; (ii) the choice of the direction of differencing at the trailing-edge station, where the irregularities/discontinuities of the flowfield have to be acknowledged; and (iii) the use of small step sizes to reveal the delicate flow features close to the trailing edge, for reasons given subsequently.

Two main sets of results are given in §3. The first concerns a thin, drooped, trailing-edge geometry, or trailing-edge flap. As the droop non-symmetry increases, so that the upper surface flow comes nearly to the verge of separating, a strong downwash, including reversed and forward flow, is promoted just beyond the trailing edge. The tongue of reversed and forward flow next reaches just ahead of the trailing edge when the upper surface flow becomes separated due to a further increase of the drooping. Thus the dividing streamline from the upper surface separation first proceeds forward beyond the trailing-edge station, but then cuts back and reattaches

to the upper surface, leaving forward flow near the surface downstream between the reattachment point and the trailing edge. The Rott–Hakkinen condition is thereby satisfied. The strength of the downwash or plunge of upper surface fluid is dictated by the strength of the forward flow leaving the lower surface, but in general it is quite intense for the immediately post-separated stage. At the same time the typical lengths involved in the downwash and ensuing reattachment processes are very small, even compared with the relatively small distance between the separation point and the trailing edge. The second set of results is for a thick trailing-edge geometry. The forward-flow condition above is irrelevant if both upper and lower surface flows are separated (see the appendix), and it is found that the pair of symmetrically disposed eddies behind a fairly thick symmetric trailing edge is gradually distorted as non-symmetry is introduced by moving the lower surface towards the fixed upper one. Eventually the downstream end of the upper eddy is pushed back towards the trailing edge, inducing an increasingly fierce plunge of upper surface fluid, which pours around the lower eddy and forces it more downstream. Further increase of the non-symmetry causes the lower eddy to be washed away, and the fierce plunge and reversal of the upper surface fluid just beyond the trailing edge make the reattachment process on the upper surface come into action as one-sided separation is reached. Subsequently, as the thin drooped configuration is retrieved, the abrupt properties noted earlier emerge again. The calculations are quite definite about the adjustment, however strong, occurring in the local flowfield in the post-separated stage, and a structural analysis (§4) of this stage as well as the pre-separated one firmly favours all the observed features above. In particular, one finding of interest is that the main lengthscale controlling the reattachment process is of the tiny relative order $\bar{A}^4$ (see also Smith 1983*a*), where, in non-dimensional terms, $-\bar{A}$ is the typical small negative skin friction induced after the upstream separation on the upper surface.

Our conclusion, then, is that catastrophic trailing-edge stall *per se* is avoided. Any difficulties encountered in treating one-sided separating flows are of a numerical rather than a conceptual nature. This, of course, provides new impetus to the use of the interactive-boundary-layer concept, since now it can continue to be used even with one-sided separation present.

Section 5 discusses the consequences of the above conclusion as far as further increases in the non-symmetry are concerned, and notes comparisons with experimental and fully numerical findings, for both laminar and turbulent flow, among other things. Also, recent studies by Burggraf (1983) and Elliott & Smith (1983) tend to favour the above conclusion. As regards notation, we use u, v to denote the velocities in the x, y Cartesian directions respectively, the thin airfoil being centred along the x-axis between $x = 0$ and $x = 1$. The velocities here and the pressure p have been non-dimensionalized with respect to u_∞^*, $\rho_\infty^* u_\infty^{*2}$, where u_∞^*, ρ_∞^* are the free-stream velocity (left to right) and density, in turn. The bulk of the investigation below applies to subsonic or supersonic laminar motions, with two-dimensionality and steadiness assumed, although subsequent generalizations are possible. The large Reynolds number $R = u_\infty^* l^*/\nu_\infty^*$ where l^* is the airfoil chord, ν_∞^* is the kinematic viscosity and the physical coordinates are l^*x, l^*y.

2. The central question of catastrophic trailing-edge stall

At the heart of things we have the triple-deck problem (Messiter 1979; Stewartson 1981; Smith 1982*a*) governing the incompressible fluid flow past a non-symmetric trailing-edge geometry, although extension to the interacting-boundary-layer concept

at finite R can be made. In the usual triple-deck form, the velocities u, v, the pressure p and the local coordinates $x-1$, y are scaled as

$$(u, v, p, x-1, y) = (R^{-\frac{3}{8}}\lambda_B^{\frac{1}{2}}U, R^{-\frac{3}{8}}\lambda_B^{\frac{3}{2}}V, R^{-\frac{1}{4}}\lambda_B^{\frac{1}{2}}P, R^{-\frac{3}{8}}\lambda_B^{-\frac{5}{4}}X, R^{-\frac{5}{8}}\lambda_B^{-\frac{3}{4}}Y), \tag{2.1}$$

for the lower deck, where $\lambda_B = 0.33206$ is the reduced skin friction of the $O(R^{-\frac{1}{2}})$ Blasius boundary layer ahead of the triple deck. Then P is independent of Y, and U, V, $P(X)$ satisfy the boundary-layer equations

$$\frac{\partial U}{\partial X} + \frac{\partial \bar{V}}{\partial \bar{Y}} = 0, \tag{2.2a}$$

$$U\frac{\partial U}{\partial X} + \bar{V}\frac{\partial U}{\partial \bar{Y}} = -P'_{\pm}(X) + \frac{\partial^2 U}{\partial \bar{Y}^2} \tag{2.2b}$$

and the boundary conditions:

$$\text{[no slip at surface]} \quad U = \bar{V} = 0 \quad \text{at} \quad \bar{Y} = 0\pm \quad \text{for} \quad X < 0, \tag{2.2c}$$

$$\text{[wake condition]} \quad P_+(X) = P_-(X),\ U \quad \text{regular in } \bar{Y} \quad \text{for} \quad X > 0, \tag{2.2d}$$

$$\text{[match with main deck]} \quad U_{\pm} \sim \pm\bar{Y} \pm F_{\pm}(X) + A_{\pm}(X) \quad \text{as} \quad \bar{Y} \to \pm\infty, \tag{2.2e}$$

$$\text{[upstream match]} \quad (U, V, P_{\pm}, A_{\pm}) \to (|\bar{Y}|, 0, 0, 0) \quad \text{as} \quad X \to -\infty, \tag{2.2f}$$

$$\text{[downstream match]} \quad P_{\pm}(\infty) = A'_{\pm}(\infty) = 0. \tag{2.2g}$$

Here (see figure 1) the subscripts $\pm$ refer to values above and below the upper and lower body surfaces $Y = F_{\pm}(X)$ respectively in $X < 0$, or above and below the line $Y = F(X)$ in $X > 0$; this line can be chosen arbitrarily subject to the convenient condition of continuity that $F(0+) = F_+(0)$, and we take $F'(0+)$ to be finite. It is assumed here that $F_+(0) = F_-(0)$ so that the body does not have an aligned steplike trailing edge. It is assumed also for convenience (see below) that the non-symmetry of the flow field, and hence of the body, is confined to the triple-deck scale in the sense that (2.2*f*, *g*) hold and $F'_{\pm}(-\infty) = 0$ (figure 1). This allows a thin or a thick symmetric or non-symmetric (e.g. drooped/flapped) blunt or sharp† trailing edge to be considered, but for the moment it deliberately avoids consideration of the effects of a significant angle of attack, for instance. Further comments concerning the influence of the angle of attack are made later. Again, the Prandtl transformation $\bar{Y} = Y - F_{\pm}(X)$, $\bar{V} = V - F'_{\pm}(X)\,U$ has been applied to yield (2.2*a–g*), while in (2.2*e*) the reduced displacement effects $A_{\pm}(X)$ are unknown in advance, as are the pressures $P_{\pm}(X)$. They are linked, however, by the pressure–displacement relation (produced in an inviscid fashion in the upper deck), which for incompressible fluid flow is

$$P_{\pm}(X) = \frac{1}{\pi}\int_{-\infty}^{\infty} \frac{A'_{\pm}(\xi)\,d\xi}{X-\xi}, \tag{2.3}$$

where the bar denotes the Cauchy principal value. For compressible fluid flow, provided that the definitions in (2.1) are suitably adjusted, the law (2.3) and (2.2*a–g*) still stand if the flow is subsonic, whereas if the flow is supersonic the only change is the replacement of (2.3) by

$$P_{\pm}(X) = -A'_{\pm}(X). \tag{2.4}$$

† We concentrate in this study on sharp non-symmetric trailing-edge geometries, to address the question of catastrophic stall. Blunt symmetric geometries have been considered recently by Werle & Verdon (1980), Korolev (1980*b*) and Vatsa, Werle & Verdon (1981).

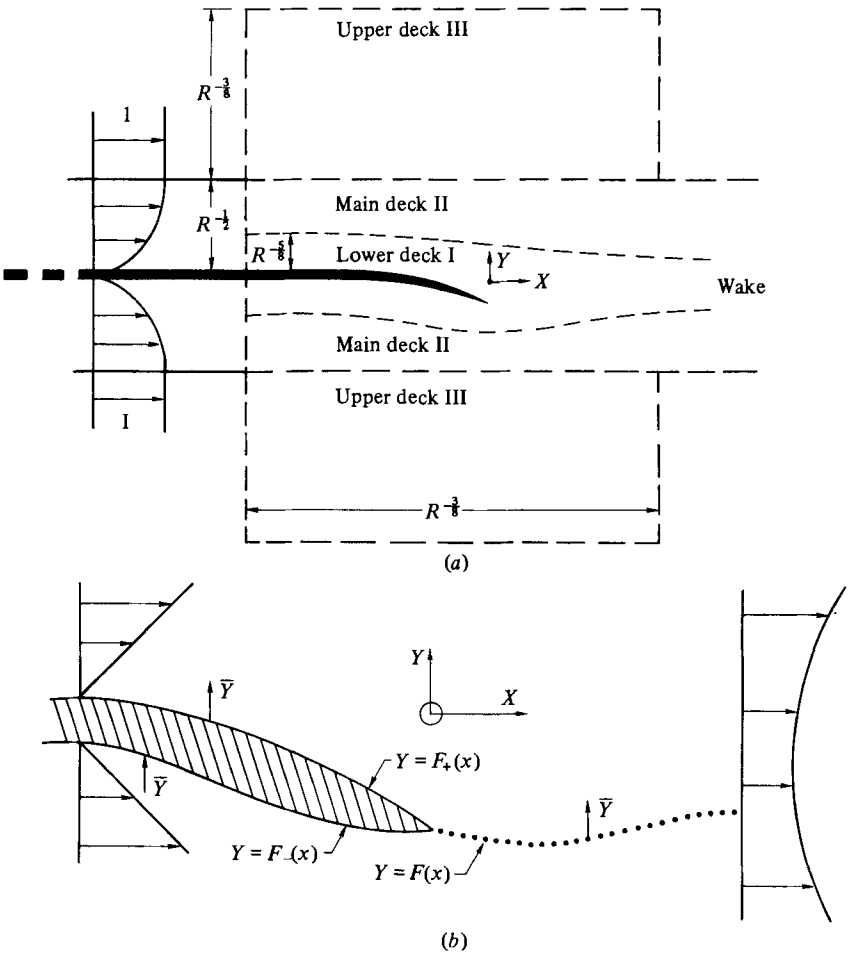

FIGURE 1. The triple-deck region near the non-symmetric trailing edge: (*a*) the general flow structure; (*b*) the lower deck I. Not to scale.

Numerical solutions and analytical properties of (2.2*a–g*) with (2.3) are to be described in §§3 and 4 in turn. Beforehand we address the central question of catastrophic trailing-edge stall, which hinges on the flow features very close to the trailing edge (on the present scale). For definiteness, suppose that the body is predominantly a thin flat plate there, in that $F'_+(0) = F'_-(0)$. Then, if the reduced skin frictions $\tau_\pm(X) = \pm\partial U/\partial Y(X, 0\pm)$ on the upper and lower surfaces are both positive, $\lambda_\pm$ say, at the onset $X = 0-$ of the trailing edge, giving forward flow there, the solution just beyond the trailing edge can be written down in terms of the Hakkinen & Rott (1965) similarity solution, for small $\bar{Y}$ at least. Thus, with Ψ denoting the stream function of U, $\bar{V}(U = \partial\Psi/\partial\bar{Y}$, $\bar{V} = -\partial\Psi/\partial X$, $\Psi = 0$ at $\bar{Y} = 0)$,

$$\left.\begin{aligned}\Psi &= X^{\frac{2}{3}}G(\eta) + \ldots,\\ P &= P(0) + X^{\frac{1}{3}}P_{\frac{1}{3}} + \ldots\end{aligned}\right\} \quad (0 < X \ll 1), \tag{2.5a}$$

where $\eta = \bar{Y}/X^{\frac{1}{3}}$ and, from (2.7*a*, *b*), $G(\eta)$ satisfies the nonlinear ordinary differential equation

$$G''' + \tfrac{2}{3}GG'' - \tfrac{1}{3}G'^2 = \tfrac{2}{3}P_{\frac{1}{3}} \tag{2.5b}$$

and the matching conditions

$$G_0(\eta) \sim \pm\tfrac{1}{2}\lambda_\pm(\eta+0)^2 \pm \frac{P_{\frac{1}{2}}}{\lambda_\pm} \quad \text{as} \quad \eta \to \pm\infty. \tag{2.5c}$$

These conditions stem from, first, the given oncoming wall-shear values $\lambda_\pm = \tau_\pm(0-)$ and, second, the necessity of effectively zero local displacement. The latter is worth noting for later use. If the '$+0$' in (2.5c) is replaced by '$+A_1$', say, then a displacement effect $-A_1 X^{\frac{1}{2}}$ is transmitted to the outer boundary condition (2.2e) (see Brown & Stewartson 1970), causing $A(X)$ to have a contribution $\propto A_1 X^{\frac{1}{2}}$, which in turn forces an effect $\propto A_1 X^{-\frac{2}{3}}$ in $P(X)$ from either of the laws (2.3) or (2.4). So there is then inconsistency with (2.5a) unless $A_1 = 0$, giving (2.5c). The solution of (2.5b, c) for $G_0(\eta)$ (and $P_{\frac{1}{2}}$) exists if

$$\lambda_\pm \geqslant 0 \tag{2.5d}$$

(for representative solutions see Brown & Stewartson 1970). It does not exist, however, if either of $\lambda_\pm$ is negative, corresponding to reversed flow on one or both surfaces at $X = 0-$, except for the special case where $\lambda_+ = -\lambda_-$, $G_0 = \frac{1}{2}\lambda_+\eta^2 + P_{\frac{1}{2}}/\lambda_+$, $U = \lambda_+ \overline{Y}$, a case which we tend to discount on physical grounds anyway. The non-existence here can be established analytically from substitution into (2.5b) of a slight perturbation to the outer constraints (2.5c): this shows that a decay towards (2.5c) is impossible then (see also Smith 1983b). In a number of interesting previous works discussing non-symmetric trailing-edge flows (Brown & Stewartson 1970; Daniels 1974; Melnik & Chow 1975; Chow & Melnik 1976; Veldman 1980; Brown & Cheng 1981; Messiter 1978; Stewartson 1974, 1981) the first appearance of separation, $\tau < 0$, on one side only of the body surface, say the upper side, so that

$$\tau_+(X_s) = 0 \quad \text{with} \quad X_s < 0 \quad \text{but } \lambda_- \text{ still positive}, \tag{2.5e}$$

has been identified or suggested as the criterion for breakdown, failure or 'catastrophic stall' of the triple-deck description, it being argued that the Rott–Hakkinen condition (2.5d) is then violated. The one-sided separation† phenomenon (2.5e) arises at an angle of attack $> \lambda_B^{\frac{8}{3}} R^{-\frac{1}{16}}\alpha_1$, $\alpha_1 = 0.47$, for the non-aligned flat plate in an incompressible fluid (Melnik & Chow 1975; Chow & Melnik 1976), for instance, and at a reduced angle $\lambda_B^{\frac{1}{3}} R^{-\frac{1}{4}}\alpha_2$, $\alpha_2 = 2.050$, in the corresponding supersonic-flow problem (Daniels 1974). Both of these problems are slight variants of (2.2a–g) with (2.3) or (2.4) of course.

Two major points arise from (2.5a–e). First and foremost, although the above argument for a catastrophic stall is tempting, it has a loophole, in that (2.5e) does *not* necessarily imply that the Rott–Hakkinen requirement (2.5d) is violated. For if the flow does separate on the upper surface at $X = X_s < 0$, then no matter how small or large $-X_s$ is, there is still room for the flow to adjust itself between $X = X_s$ and $X = 0$ to ensure that (2.5d) is satisfied. This view receives extra support from the fact that, once separation takes place at $X = X_s < 0$, the boundary-layer equations become parabolic in the negative X-direction during the reversed flow for $X > X_s$,

† By contrast, if two-sided separation is present, as in Werle & Verdon (1980), Korolev (1980b), Vatsa *et al.* (1981), Ruban & Sychev (1979), Smith & Merkin (1982), and also §3, then the expansion (2.5a) no longer applies. Instead an essentially uniform reversed stream is present in the wake as $X \to 0+$ for small $\overline{Y}$. This forces Blasius-like $O(-X)^{\frac{1}{2}}$ reversed sublayers on the body surfaces in $X < 0$ for small $|X|$ and an $O(-X)^{-\frac{1}{2}}$ dependence in the negative skin frictions $\tau_\pm(X)$ as $X \to 0-$, so that in effect $\lambda_\pm$ are then both infinitely negative. See the appendix.

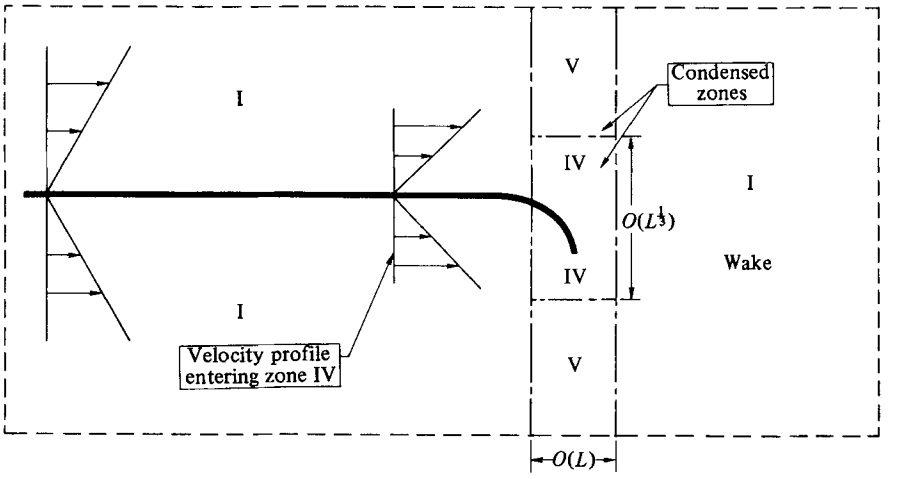

FIGURE 2. Schematic diagram (not to scale) of the 'condensed' trailing-edge region.

until the flow becomes totally forward again further downstream. So information can be transmitted upstream through the reversed flow in $X > X_s$, thus providing a strong local mechanism by which the condition (2.5*d*) at $X = 0-$ can make its presence felt upstream, and in particular force the skin friction $\tau_+(X)$ to become positive again in $X_s < X_r < X < 0$, in principle. Indeed the above outlines the main idea of the present work, that if (2.5*e*) holds then a *reattachment* always occurs before the trailing edge, to make λ_+, positive in compliance with (2.5*d*).

The second point here is that the pressure–displacement law, unless it is particularly bizarre, really plays no significant part in deciding the main issue of catastrophic stall, i.e. the satisfaction of (2.5*a–d*). Whether (2.3) or (2.4) holds, or, indeed, if the flow is hypersonic, the local flow behaviour must still have the form (2.5*a–d*) near the trailing edge, with the condition (2.5*c*) signifying effectively zero displacement effect there. In addition, if the upstream separation distance $-X_s$ is at all small, then again the pressure–displacement law is largely irrelevant (see also §4) because, as with (2.5*c*), this most sensitive part of the flowfield is close to the trailing edge where the pressure–displacement law always reduces to the constraint of zero local displacement, to leading order. It does not provide a strong enough mechanism, comparable to that described in the previous paragraph, for the upstream transmission of information locally near the trailing edge. In a sense the particular form of the pressure–displacement law is a secondary matter, therefore, even an unnecessary complication, as regards the main question of catastrophic stall.

In consequence, as well as addressing the triple-deck problem of (2.2*a–g*), (2.3) subsequently, we study also the simpler 'condensed problem' (figure 2) which arises from (2.2*a–g*), (2.3) or (2.4) as follows. Suppose that the streamwise and lateral scales of the trailing-edge non-symmetry in (2.2*e*) are both small, of order L, $L^{\frac{1}{3}}$, respectively, relative to the lower-deck coordinates X, Y, so that

$$F_\pm(X) = L^{\frac{1}{3}}\tilde{F}_\pm\left(\frac{X}{L}\right), \tag{2.6}$$

say. Then for most of the flowfield (zones I in figure 2), effectively $F_\pm(X) = 0$ in (2.2*e*) and so there, to within $O(L^{\frac{2}{3}})$, (2.2*a–g*), (2.3) reduce to the symmetric flat-plate problem, numerical solutions for which are given by Jobe & Burggraf (1974), Melnik & Chow (1975) and Veldman & van de Vooren (1975) and others. The motion there

stays attached, with the skin friction $\tau_\pm(X) \to \mu_0 > 0$ as $X \to 0-$, the pressure $P_\pm(X) \to \pi_0 < 0$ as $X \to 0\pm$, $P'_\pm(0-)$ is finite but $P'(X) \propto X^{-\frac{1}{2}}$ as $X \to 0+$, as in (2.5a), to leading order. Values for the $O(1)$ constants μ_0, π_0 are given in the above references. Closer to the trailing edge, however, in zone IV on the condensed scales $X = L\hat{X}$, $\overline{Y} = L^{\frac{1}{3}}\mu_0^{-\frac{1}{3}}\hat{Y}$, the flow properties have the development

$$[U, V, P] = [L^{\frac{1}{3}}\mu_0^{\frac{2}{3}}\hat{U}(\hat{X}, \hat{Y}), L^{-\frac{1}{3}}\mu_0^{\frac{1}{3}}\hat{V}(\hat{X}, \hat{Y}), \pi_0 + L^{\frac{2}{3}}\mu_0^{\frac{4}{3}}\hat{P}(\hat{X})] + \ldots. \tag{2.7}$$

See Smith *et al.* (1981) for a discussion of the wide range of validity of the description (2.7) for flow over humps; a similar approach shows that the ultimate conclusion (2.9) below holds also if the incident skin friction λ_B is reduced. In (2.7) the orders for U, V are inferred from the local $O(1)$ skin friction and from mass conservation, and the order of P then follows from the momentum balance. From (2.2a, b) $\hat{U}$, $\hat{V}$, $\hat{P}$ therefore satisfy

$$\frac{\partial \hat{U}}{\partial \hat{X}} + \frac{\partial \hat{V}}{\partial \hat{Y}} = 0, \tag{2.8a}$$

$$\hat{U}\frac{\partial \hat{U}}{\partial \hat{X}} + \hat{V}\frac{\partial \hat{U}}{\partial \hat{Y}} = -\hat{P}'(\hat{X}) + \frac{\partial^2 \hat{U}}{\partial \hat{Y}^2}, \tag{2.8b}$$

while the appropriate boundary conditions are now

$$\hat{U} = \hat{V} = 0 \quad \text{at} \quad \hat{Y} = 0\pm \quad \text{for} \quad \hat{X} < 0, \tag{2.8c}$$

$$\hat{P}_+(\hat{X}) = \hat{P}_-(\hat{X}), \quad \hat{U} \text{ regular in } \hat{Y} \quad \text{for} \quad \hat{X} > 0, \tag{2.8d}$$

$$\hat{U}_\pm \sim \pm\hat{Y} \pm \hat{F}_\pm(\hat{X}) \quad \text{as} \quad \hat{Y} \to \pm\infty, \tag{2.8e}$$

$$(\hat{U}, \hat{V}, \hat{P}'_\pm(\hat{X})) \to (|\hat{Y}|, 0, 0) \quad \text{as} \quad \hat{X} \to -\infty, \tag{2.8f}$$

where $\hat{F}_\pm(\hat{X}) \equiv \mu_0^{\frac{1}{3}}\tilde{F}_\pm(\hat{X})$. Here (2.8$c, d$) correspond to (2.2$c, d$), but (2.8$e, f$) require further comment. First, if a displacement term $\hat{A}_\pm(\hat{X})$ is added to (2.8e) then its effect is felt throughout the $O(L)$ by $O(1)$ zones V (figure 2) above and below the concentrated zone IV; so the induced displacement $A_\pm$ in (2.2f) is $\propto L^{\frac{1}{3}}\hat{A}_\pm(\hat{X})$; but then the pressure–displacement law (2.3) or (2.4) forces a pressure response of order $L^{-\frac{2}{3}}\mathrm{d}\hat{A}_\pm/\mathrm{d}\hat{X}$, contradicting (2.7) and the momentum balance; hence $\hat{A}_\pm(\hat{X}) \equiv 0$. So (2.8$e$) satisfies both the match with the symmetric shear $\partial U/\partial Y \sim \mu_0$ in I and the pressure–displacement law (2.3) or (2.4). The argument is similar to that used previously for (2.5c). Secondly, (2.8f) matches to the incoming symmetric shear μ_0 upstream in I, but it allows non-zero pressure levels, of order $L^{\frac{2}{3}}$ from (2.7), to emerge there from the condensed zone. These levels coincide with the pressure-perturbation levels throughout I and need be reduced to zero only as $|X| \to \infty$ in I. On the other hand, the local pressure gradient in IV is large, $O(L^{-\frac{1}{3}})$ from (2.7), as compared with the $O(1)$ gradient in I, so that the values $P'_\pm(-\infty) = 0$ are required for consistency.

The condensed problem (2.8a–f) is still controlled by the behaviour (2.4a–c) at $\hat{X} = 0+$ subject to the redefinitions (2.7) and $\hat{\tau}(\hat{X}) = \partial\hat{U}/\partial|\hat{Y}|\,(\hat{X}, 0)$, $\hat{\tau}_\pm(0-) = \hat{\lambda}_\pm$. For (2.5$c$) is independent of the pressure–displacement law (2.3), (2.4) anyway, and so in particular it applies to the condensesd problem for which in effect (2.3) or (2.4) is replaced by the simpler law

$$A_\pm(X) \equiv 0, \tag{2.9}$$

because of (2.8e). Therefore the central question of catastrophic stall raised by (2.5d, e) does remain present as required. However, the law (2.9) yields two advantages. The first is that the flow problem becomes entirely parabolic in the $+X$

direction ahead of any separation (Smith 1976), so that, numerically, multiple sweeping of the flow there is not required. The upper and lower surface flows remain independent up to separation, which, as with (2.3), (2.4) is always regular. The second advantage is that (2.9), the 'condensed problem', puts the inviscid pressure–displacement law aside, as it should be (see earlier comments) in the central question of catastrophic stall. Thereby it allows a much closer investigation to be made into the idea of the present work that, when $-X_s$ is small at least, the resolution of (2.5*e*) versus (2.5*d*) occurs by means of a reattachment forced by the upstream influence within the boundary-layer equations alone, and that catastrophic stall does not occur.

3. Numerical method and solution

A finite-difference numerical treatment was adopted. Although for reasons just stated we attended mainly to the condensed problem, the treatment was developed for, and so is described in terms of, the triple-problem primarily, with the condensed problem then emerging as a special case.

The method is an extension of Smith & Merkin's (1982) technique. In summary, the transformation $X = \tan \bar{X}$ is used to handle the range $(-\infty, \infty)$ of X by calculation in $-\frac{1}{2}\pi \leqslant \bar{X} \leqslant \frac{1}{2}\pi$ and to assemble grid points near the trailing edge. Then, for each sweep of the flowfield, the upper surface layer $\bar{Y} \geqslant 0$ is marched forward from (2.2*f*) at $\bar{X} = -\frac{1}{2}\pi$ to $\bar{X} = 0-$ by solving three first-order equations for Ψ, U, $\partial U/\partial \bar{Y}$ from (2.2*a*, *b*), with two boundary conditions on U, $\partial U/\partial \bar{Y}$ nominally as $\bar{Y} \to \infty$ from (2.2*e*) and two on Ψ, U at $\bar{Y} = 0$ from (2.2*c*). The lower surface layer $\bar{Y} \leqslant 0$ is marched similarly up to the trailing edge. In general, that leaves P_+, P_- unequal at $X = 0$, in subsequent violation of (2.2*d*) at that stage. This difficulty is resolved simply by calculating the average pressure $P_{\mathrm{av}} = \frac{1}{2}(P_+(0) + P_-(0))$, multiplying all the latest $A_\pm$ values by $P_\mp(0)/P_{\mathrm{av}}$ and afterwards setting $P_\pm(0)$ equal to P_{av}. The wake $\bar{X} > 0$ can then be marched forward with two boundary conditions now on U, $\partial U/\partial \bar{Y}$ nominally as $\bar{Y} \to \pm\infty$ at each $\bar{X}$-station and subject to the unknown pressure $P_\pm$, to which P_- is equated in retrospect for (2.2*d*). The next sweep then starts at $\bar{X} = -\frac{1}{2}\pi$. At each station the local Veldman (1980*a*, *b*) technique, modified because $X = \tan \bar{X}$, is applied for updating $P_\pm$, $A_\pm$ at $\bar{X}$, given (2.3) and a global guess for $A_\pm$. The nonlinearity of (2.2*a*, *b*) in centred-difference form is treated with Newton iteration followed by Gaussian elimination and superposition to fix the incremental pressures locally. Deliberately a limited number of Newton iterations is permitted per station, the solution there then being stored so that the iterative tolerance (typically 10^{-7}) is achieved in the later sweeps by taking the latest stored values of the solution as initial guesses. Again, since $A_\pm$ grows like $X^{\frac{1}{3}}$ as $X \to \infty$ (see (3.4*a–d*) below) in the triple-deck problem we worked in terms of the modified variables $P_{s\pm}$, $A_{s\pm}$ of Smith & Merkin (see their (2.11*b*)) to allow for the growth. In later calculations we also used a stretching in the $\bar{Y}$-coordinate, coupled with the new transformation $X = (\tan \bar{X})^3$ $[-\frac{1}{2}\pi \leqslant \bar{X} \leqslant \frac{1}{2}\pi]$. This was done partly to accommodate the similarity form (2.5*a–c*) and its counterpart

$$\Psi = \Psi_0(\bar{Y}) - P_{\frac{1}{3}} X^{\frac{2}{3}} U_0(\bar{Y}) \int_{\pm\infty}^{\bar{Y}} \frac{\mathrm{d}Y_1}{(U_0(Y_1))^2} + \ldots \quad (\bar{Y} \gtrless 0) \tag{3.1}$$

for $\bar{Y} = O(1)$, as $X \to 0+$, where $U_\pm = U_0(\bar{Y})$, $\Psi_\pm = \Psi_0(\bar{Y})$ give the solution profiles at $X = 0-$, and partly to assemble the grid points immediately upstream of $X = 0$ in line with the analysis of §4. The scheme converges in 10–20 sweeps typically.

For the condensed problem the matter is simpler, because effectively (2.9) replaces

(2.3), and (2.9) on its own induces no upstream influence. So without reversed flow present only one sweep of the flowfield is required. Techniques similar to the above are applicable. The upper and lower surface layers are again marched up to the trailing edge, but now with $\hat{P}_\pm - \hat{P}_\pm(-\infty)$ being determined at each station. Since the requirement $\hat{P}_+(0) = \hat{P}_-(0)$ holds, the value of $\hat{P}_+(-\infty) - \hat{P}_-(-\infty)$ can immediately be found, while the pressure level $\hat{P}_+(-\infty)$ remains unknown, in keeping with the comments of §2. Then the wake solution is derived by forward marching, and the solution terminates with the property

$$\hat{P}_\pm(\hat{X}) \propto \hat{X}^{\frac{2}{3}} \quad \text{as} \quad \hat{X} \to \infty \tag{3.2}$$

($\overline{X} \to \frac{1}{2}\pi -$) automatically emerging downstream. Here (3.2) merges the condensed-flow solution in IV in figure 2 with that of the essentially aligned flat plate outside in I as $X \to 0+$. Thus Rott–Hakkinen forms apply both as $\hat{X} \to 0+$ and as $\hat{X} \to \infty$. For these forward-flow calculations the Newton iterations must be continued at each station until the iterative tolerance is satisfied, to avoid sweeping.

The above applies if there is no reversed flow. If flow reversal does occur, however, then, since the boundary-layer equations become parabolic in the $-X$-direction locally, an iterative approach allowing information to be transmitted in the $-X$-direction there is essential. Although some approximate numerical treatments do apparently allow the solution to be marched foward without any such transmission of information, they contradict the physics and mathematics of the reversed-flow situation: this is either by actually changing the governing equations, as in the Reyhner & Flügge-Lotz (1968) approximation, or by using difference approximations which appear stabilizing for finite grid sizes and/or forward flow but which surely cannot be stable in the required limit of zero step size for reversed flow, as in the Du-Fort–Frankel and extended backward-differencing schemes (Dijkstra 1978; Dijkstra & Veldman 1980). In some flow problems the difficulty seems not too crucial because the reversed flow does remain passive and small numerically. In the present trailing-edge separating flow, by contrast, the role of the reversed flow is vital, especially near the trailing edge, in deciding the issue of stall. Accordingly we adopted first a windward-differencing approach to incorporate the upstream influence of any reversed flow. To date the approach has been applied only to the condensed problem and is considered in that context, although it applies equally well to the triple-deck problem also. Wherever $\hat{U} < 0$ at a station $\hat{X}$ the term $\hat{U}\partial\hat{U}/\partial\hat{X}$ in (2.8*b*) is replaced by the appropriate forward difference involving the unknown $\hat{U}^{(n)}$ at $\hat{X}$ and the value $\hat{U}^{(n-1)}$ at $\hat{X} + \delta\hat{X}$ given from the previous sweep of the flowfield, where (n) refers to the value at the current nth sweep and $\delta\hat{X}$ is the local step size in $\hat{X}$. We start with $\hat{U}^{(0)} \equiv 0$, say. Elsewhere the original forward-marching method remains intact. The scheme is similar to, but not identical with, for example, that of Carter & Wornom (1975; see also Carter 1974, 1979). It remains stable, and the crucial backflow effect enters the solution sweep by sweep until overall convergence is obtained in about 10–15 sweeps, depending on the grid dimensions used. That scheme still essentially glosses over one essential aspect, the feature that $\partial\hat{\Psi}/\partial\overline{X} = -\hat{V}\,\mathrm{d}X/\mathrm{d}\overline{X}$ and $\mathrm{d}\hat{P}/\mathrm{d}\overline{X}$ are discontinuous across $\hat{X} = 0$ (from (3.1), (2.5*a–c*) with '^' overlaid and $X = (\tan\overline{X})^3$). Therefore a number of computational trials were made, with varying degrees of success, to accommodate that feature. In the final modified scheme, the terms $\hat{V}\partial\hat{U}/\partial\hat{Y}$ and the pressure gradient, at the station $\hat{X} = 0$ only, are also represented completely by forward differences whenever $\hat{U} < 0$. This step involves adding in the appropriate correction contributions from the stations $\hat{X} = -\delta\hat{X}$, 0, $\delta\hat{X}$ retrospectively, using previously calculated values, to make the eventual converged solution

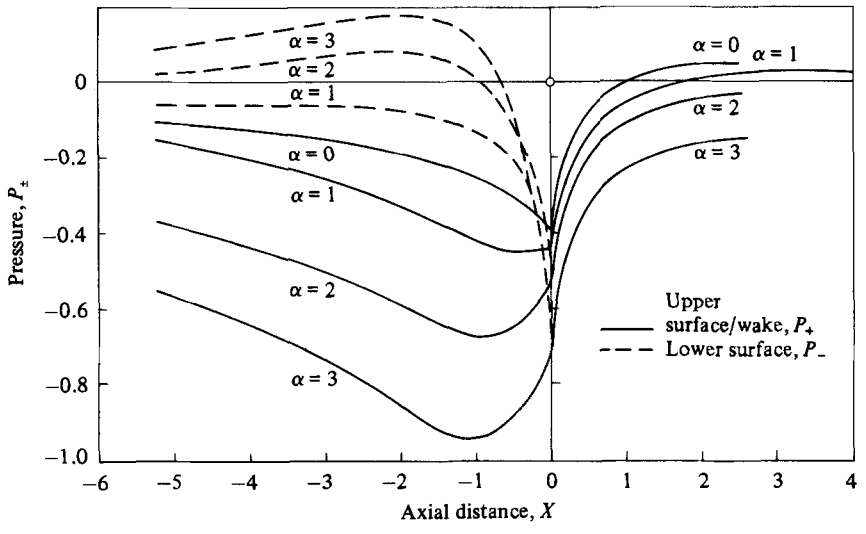

(*a*)

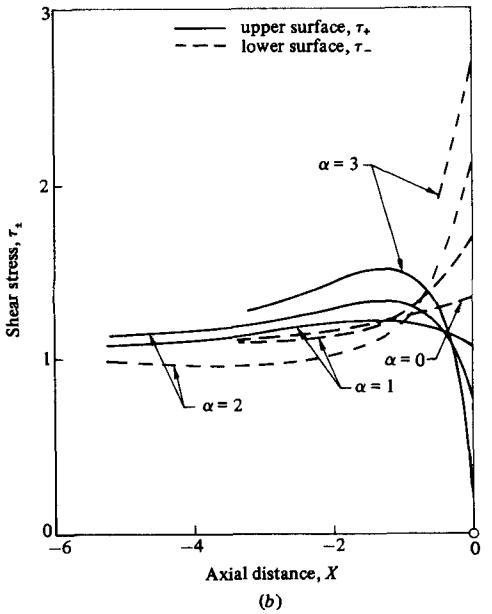

(*b*)

FIGURE 3. Solutions of the triple-deck for a drooped trailing edge, or trailing-edge flap: (*a*) pressure distributions; (*b*) surface shear stress; both versus X.

allow for the irregularities at the trailing edge station. The test on the condition $\hat{U} \gtrless 0$ here is placed at $\hat{X} = \delta\hat{X}$ for consistency, since otherwise the same momentum balance could be used twice, in the determination of the solution at $\hat{X} = 0$ and at $\hat{X} = \delta\hat{X}$. This placing further serves to inform the upper surface flow ahead of the trailing edge, sweep by sweep, that forward flow is essential at $\hat{X} = 0$ if the lower surface flow is still attached, from (2.5*a–d*). The modified scheme therefore allows for the irregularities of (3.1), (2.5*a–c*) as well as for the backflow, and so throughout it seems formally correct in the limit of zero step size. Certain other modifications were tested, including three-point forward differencing and the use of $\hat{U}^{(n-1)}$ at $\hat{X}$ instead of $\hat{U}^{(n)}$ for the

reversed flow, but these had negligible effect on the final results. Typically (see also the grid test below) we took 101 or 201 streamwise steps, 81 or 161 laterally, with outer boundaries at ± 8 and a Newton iterative tolerance of 10^{-7}.

Concerning the triple-deck problem (2.2*a–g*), (2.3), numerical solutions are presented in figure 3 for the shapes

$$F_{\pm}(X) = \frac{-\alpha}{L^2 + (X - \sqrt{\frac{1}{3}}L)^2} \tag{3.3}$$

corresponding to a thin non-symmetric drooped trailing edge or trailing-edge flap, with $L = 1$ and for various values of $\alpha \geqslant 0$. As a check, for $\alpha = 0$ in figure 3 the aligned flat-plate solution noted earlier is retrieved satisfactorily. For the positive values of α shown, the upper surface pressure P_+ first falls gradually in $X < 0$ (figure 3*a*), inducing a tendency towards firm attachment upstream ($\tau_+ \uparrow$) (figure 3*b*) before the opposite occurs closer to the trailing edge, where P_+ rises and τ_+ falls quickly. This is sensible physically, as are the eventual rise and fall in P_-, τ_- upstream before the favourable pressure gradient and rise in τ_- emerge nearer $X = 0-$. Beyond the trailing edge the pressure first increases fast (cf. (2.5*a*)), then it attains a positive maximum, and far downstream returns to its original value of zero. The farfield forms of P, A as $X \to \infty$ are

$$A_{\pm} = \begin{cases} \gamma_1 X^{\frac{1}{3}} \pm \gamma_2 X^{-\frac{1}{2}} + \ldots & \text{as} \quad X \to +\infty, \quad (3.4a) \\ O(|X|^{-1}) & \text{as} \quad X \to -\infty, \quad (3.4b) \end{cases}$$

$$P_{\pm} = \begin{cases} (\tfrac{1}{3})^{\frac{3}{2}} \gamma_1 X^{-\frac{2}{3}} + \ldots & \text{as} \quad X \to +\infty, \quad (3.4c) \\ -(\tfrac{1}{3})^{\frac{3}{2}} 2\gamma_1 |X|^{-\frac{2}{3}} \mp \tfrac{1}{2}\gamma_2 |X|^{-\frac{3}{2}} + \ldots & \text{as} \quad X \to -\infty, \quad (3.4d) \end{cases}$$

from (2.2*a–g*), (2.3), where $\gamma_1 = 0.892$ (for an alternative see Smith 1983*b*) but γ_2 is an unknown constant dependent upon the entire flow solution for X finite. In figure 3(*a*) the pressure difference shown, $P_+ - P_-$, is responsible for the lift produced by viscous action around the non-symmetric trailing edge, as compared with the inviscid lift which is zero. As the droop factor α increases, the lower surface skin friction of figure 3(*b*) at the trailing edge $\tau_-(0) = \lambda_-$ increases, but the upper surface value $\tau_+(0) = \lambda_+$ decreases, and the results suggest the onset of separation at $\alpha \approx 3.5$. At this juncture, therefore, we switched attention to the issue of catastrophic stall as addressed more directly by the condensed problem.

For the condensed problem (2.8*a–e*), the trailing-edge geometry was taken as

$$\left.\begin{aligned} \hat{F}_+(\hat{X}) &= -\frac{\hat{\alpha}_1}{1 + (\hat{X} - \sqrt{\frac{1}{3}})^2}, \\ \hat{F}_-(\hat{X}) &= -\frac{\hat{\alpha}_2}{(1 + (\hat{X} - \sqrt{\frac{1}{3}})^2)} + \tfrac{3}{4}(\hat{\alpha}_2 - \hat{\alpha}_1) \end{aligned}\right\} \tag{3.5}$$

for various values of $\hat{\alpha}_1 (> 0)$, $\hat{\alpha}_2$. Here (3.5) gives a thin or a thick symmetric or non-symmetric, e.g. drooped/flapped, trailing edge. The connection with (3.3) for the corresponding triple-deck problem is achieved by taking L small with α of order $L^{\frac{7}{3}}$. When $\hat{\alpha}_2 = \hat{\alpha}_1$ the geometry is the thin drooped plate again, and figure 4 gives the results for that case (including a sample check on the effects of grid size) as $\hat{\alpha}_1$ is increased from zero. For $\hat{\alpha}_1 = \hat{\alpha}_2 = 0$ the plate is flat and the condensed solution is trivial: $\hat{U}_{\pm} \equiv |\hat{Y}|$, $\hat{P} \equiv 0$ for all $\hat{X} < 0$ while $\hat{U} \equiv \hat{X}^{\frac{1}{3}} G_0'(\hat{\eta})$, $\hat{P} \propto \hat{X}^{\frac{2}{3}} (\lambda_{\pm} \equiv 1)$ for all

$\hat{X} > 0$. The numerical results achieve this form satisfactorily in figure 4. Then for $\hat{\alpha}_1 = \hat{\alpha}_2$ positive the upper and lower surface pressures $\hat{P}_\pm$ respectively increase and decrease monotonically (figure 4*a*), and $\hat{\tau}_\pm$ do the opposite (figure 4*b*), provided there is no separation. There is some relation with the earlier triple-deck results, but without the secondary issue of upstream influence forcing the initial upstream trends of figure 3. The onset of upper-surface separation is reached now at $\hat{\alpha}_1 = \hat{\alpha}_c \approx 2.42$, where $\hat{\lambda}_+ \to 0+$. Solutions are also shown for the post-separated configuration for larger values (up to 4) of $\hat{\alpha}_1 = \hat{\alpha}_2$, with $\hat{\lambda}_- > 0$ and figure 4 indicating what is believed to be the resolution of the dilemma between (2.5*d*, *e*): a reattachment takes place between $X = X_s < 0$ and $X = 0-$ (see figure 4*b*, *c*).

The typical lengths involved in the reattachment processes just before the trailing edge were observed to be very small numerically (e.g. figure 4*c*). They hardly show up at all on a conventionally sized plot of the entire flow solution, a feature which fits in well with the subsequent analysis of the post-separated situation, in §4, in fact. Further, the extreme grid refinement, particularly in the $\hat{X}$-direction, proved necessary to track the solution in the vicinity of the trailing edge, although virtually all the rest of the solution could be fixed accurately with a less refined grid. This again ties in with §4 below. It is worth remarking here that often with a less refined grid or before iterative convergence was achieved the Rott–Hakkinen condition (2.5*d*) could be violated by the numerical solution without causing any apparent breakdown; but, as convergence approached and/or the grid was refined, the value of $\hat{\lambda}_+$ then increased and eventually became positive owing to a small abrupt pressure drop locally (figure 4*c*), with the other values of $\hat{\tau}_+(\hat{X})$ altering relatively little throughout.

Another view of the proposal concerning reattachment is provided by the results in figure 5 for $\hat{\alpha}_1 = 4$ kept fixed, so that upper-surface separation in $\hat{X} < 0$ is guaranteed, but with $\hat{\alpha}_1 \geqslant \hat{\alpha}_2 \geqslant -\hat{\alpha}_1$. The lower surface flow is then also separated if $\hat{\alpha}_2 < -\hat{\alpha}_c$, in which case the account (2.5*a–d*) does not apply as it is replaced by that in the appendix, and the question of catastrophic stall does not arise. If $\hat{\alpha}_2 > -\hat{\alpha}_c$, however, there is no lower surface separation and the matter of catastrophic stall can be readdressed. Gradually increasing $\hat{\alpha}_2$ from $-\hat{\alpha}_1$ to $\hat{\alpha}_1$ corresponds to gradually changing the trailing-edge geometry from a nearly blunt symmetric shape to the non-symmetric thin drooped plate. The transition of the numerical solutions for pressure and skin friction in figure 5 (*a–b*) as $\hat{\alpha}_2$ increases is physically sensible, especially in view of the corresponding development of the streamline patterns shown in figures 6 (*a–e*). The emergence of the upper-surface reattachment as $\hat{\alpha}_2$ passes through the value $\hat{\alpha}_2 = -\hat{\alpha}_c$ seems almost inevitable. The two recirculating eddies tend to be rotated towards the upper surface and distorted due to the extra non-symmetry, the increased strength of the oncoming lower-surface flow and the resultant draw of the upper-surface fluid towards the lower. Eventually the lower eddy disappears completely.

The trends of the above solutions, including the fairly abrupt reattachment phenomenon, tie in closely with the following description of the flow properties for the pre- and post-separation stages. The description applies equally well to the triple-deck or the condensed problem.

4. Analysis of the pre- and post-separation properties

4.1. *General comments*

Below we consider the structures of the non-symmetric trailing-edge motion when: (*a*) the motion is pre-separated, with forward flow along both surfaces, but the upper

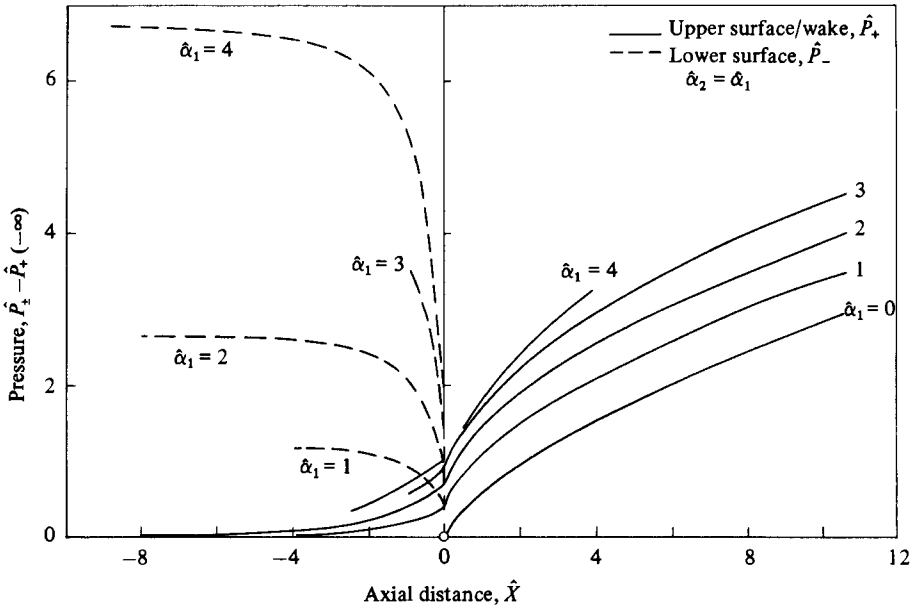

(*a*)

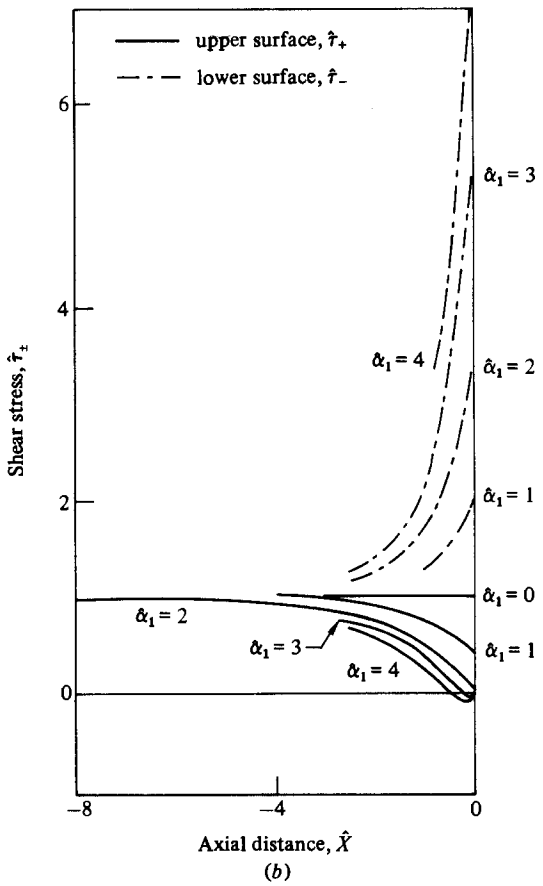

(*b*)

FIGURE 4 (*a*, *b*). For caption see facing page.

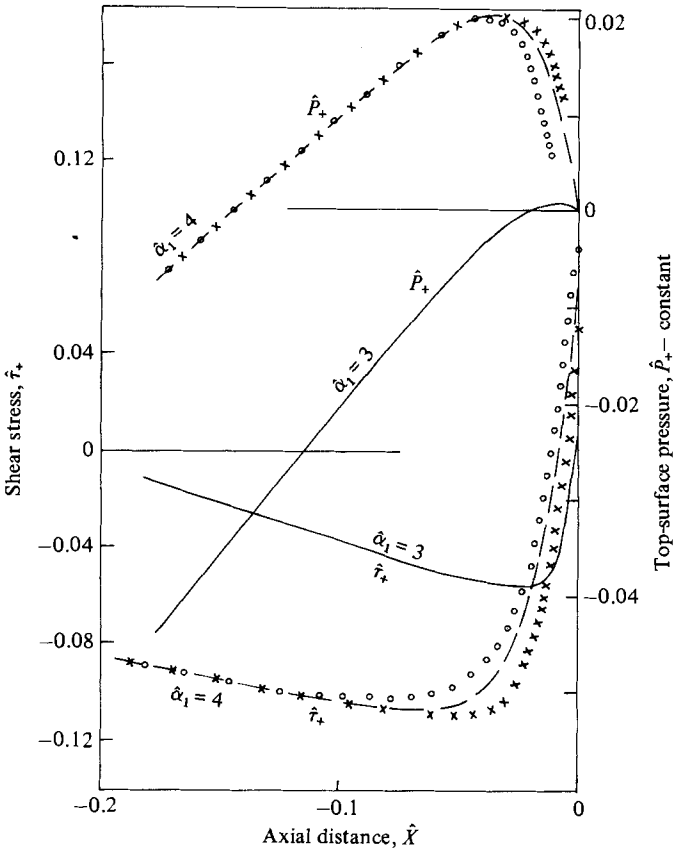

(*c*)

FIGURE 4. Solutions of the condensed problem for a thin drooped/flapped trailing edge ($\hat{\alpha}_1 = \hat{\alpha}_2$): (*a*) pressure; (*b*) surface shear stress; (*c*) close-up view for the separated cases $\hat{\alpha}_1 = 3$, 4 near the trailing edge, including for $\hat{\alpha}_1 = 4$ the effects of grid refinement (which elsewhere are negligible graphically). (o o o, 51 gridpoints in $\bar{X}$ and 41 gridpoints in $\hat{Y}$; – – –, 101 and 81; × × ×, 201 and 161.) See also figure 6.

surface skin friction is small at the trailing edge; and (*b*) the motion is post-separated with separation present on one surface only, as in (2.5*e*), just ahead of the trailing edge. The structures hold quite generally, for the triple-deck or the condensed problem, and for the flat plate at angle of attack as well as for the trailing-edge geometries studied hereto. They are also independent of the pressure–displacement law and so concern both subsonic and supersonic flow in particular. To be specific below we use the triple-deck problem as the basis.

4.2. *Pre-separated flow*

Suppose that $\alpha = \alpha_c - \Delta$, where α_c is the $O(1)$ separation value of α, giving $\lambda_+ = 0$, while Δ is small but positive. Then typically λ_+ is small and $O(\Delta)$, $\lambda_+ = \Delta\tilde{\lambda}_+$ say. Over most of the flowfield the solution is that for $\alpha = \alpha_c$ (the special case considered by Daniels (1974) with which our work is consistent when $\Delta = 0$) but slightly perturbed by an amount $O(\Delta)$. Near the trailing edge, however, the perturbation due to Δ is not small on a tiny lengthscale $O(\Delta^{\frac{3}{4}})$ in X. If $X = \Delta^{\frac{3}{4}}\tilde{X}$ then the flow solution subdivides essentially into two subzones SP_1, SP_2 for $\tilde{X}$ finite and positive (figure 7*a*), with

$$P = \Delta^{\frac{1}{4}}\tilde{P}(\tilde{X}) + \ldots. \tag{4.1}$$

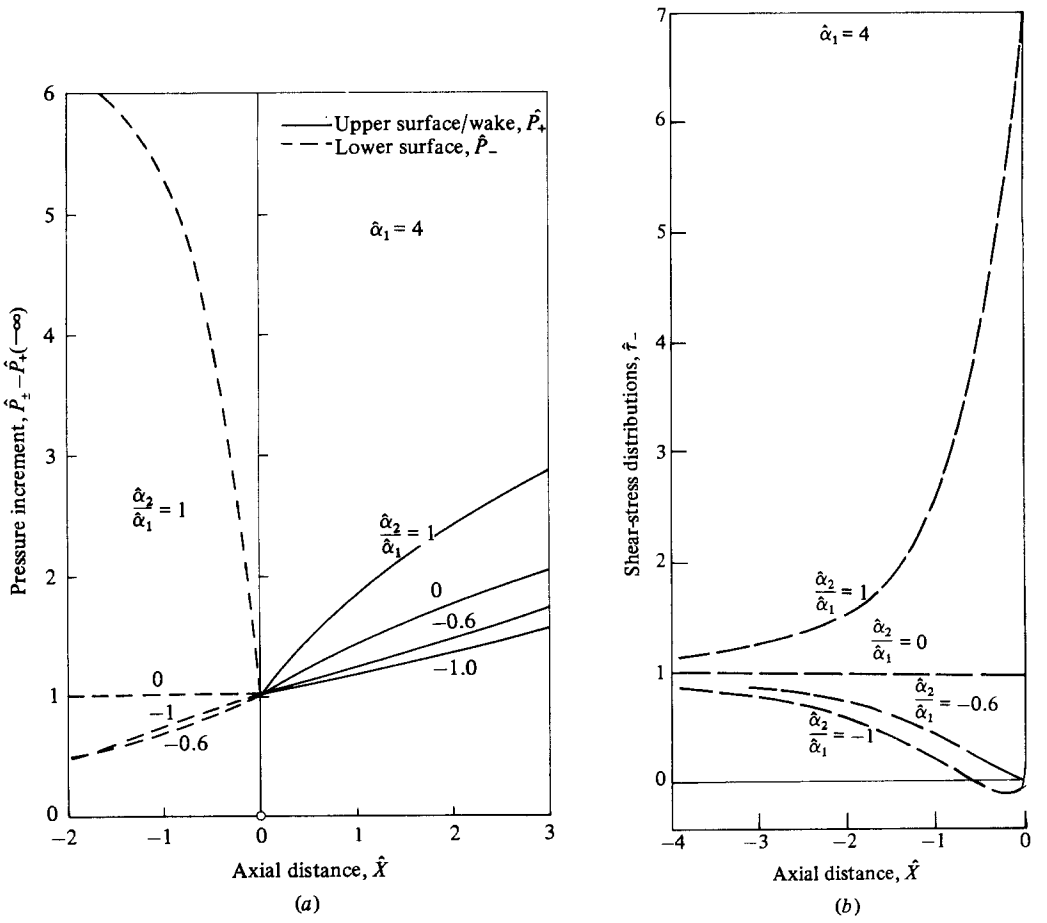

FIGURE 5. The condensed problem for thick trailing edges with $\hat{\alpha}_1 = 4$ fixed and $\hat{\alpha}_2$ varying: (*a*) the pressure increment; (*b*) the surface shear stress. See also figure 6.

Subzone SP_1 has

$$\Psi = \Delta^3 \tilde{\Psi}_1 + \ldots, \quad U = \Delta^{\frac{3}{2}} \tilde{U}_1 + \ldots, \quad \overline{Y} = \Delta^{\frac{3}{2}} \tilde{Y}_1, \tag{4.2}$$

and closely surrounds the trailing edge for $X > 0$, it being assumed that λ_- is $O(1)$. Hence $\tilde{\Psi}_1$, $\tilde{U}_1$ satisfy the viscous shear-layer equations and boundary conditions

$$\tilde{U}_1 = \frac{\partial \tilde{\Psi}_1}{\partial \tilde{Y}_1}, \quad \tilde{U}_1 \frac{\partial \tilde{U}_1}{\partial \tilde{X}} - \frac{\partial \tilde{\Psi}_1}{\partial \tilde{X}} \frac{\partial \tilde{U}_1}{\partial \tilde{Y}_1} = \frac{\partial^2 \tilde{U}_1}{\partial \tilde{Y}_1^2}, \tag{4.3a}$$

$$\tilde{\Psi}_1 \sim -\tfrac{1}{2}\lambda_- \tilde{Y}_1^2 + o(1) \quad \text{as} \quad \tilde{Y}_1 \to -\infty, \tag{4.3b}$$

$$\frac{\partial \tilde{U}_1}{\partial \tilde{Y}_1}(\tilde{X}, \infty) = 0, \tag{4.3c}$$

with no pressure force, from (2.2*a–g*) essentially, and a similarity starting form. The appropriate solution is

$$\tilde{\Psi}_1 = \tilde{X}^{\frac{2}{3}} G_0(\tilde{\eta}), \quad \tilde{U}_1 = \tilde{X}^{\frac{1}{3}} G_0'(\tilde{\eta}), \quad \tilde{\eta} \equiv \frac{\tilde{Y}_1}{\tilde{X}^{\frac{1}{3}}}, \tag{4.4}$$

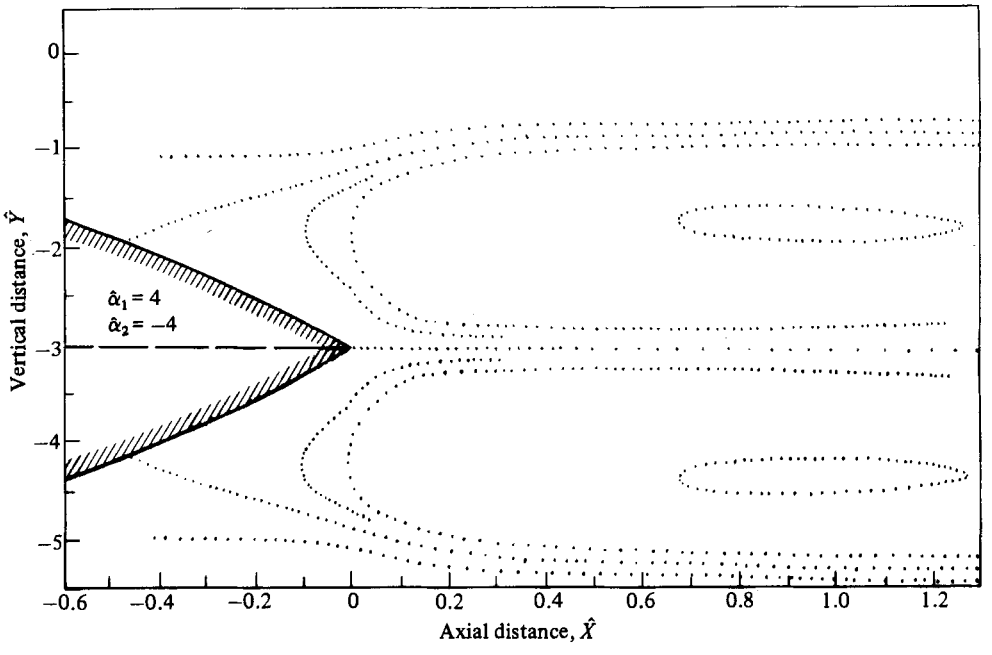

(*a*)

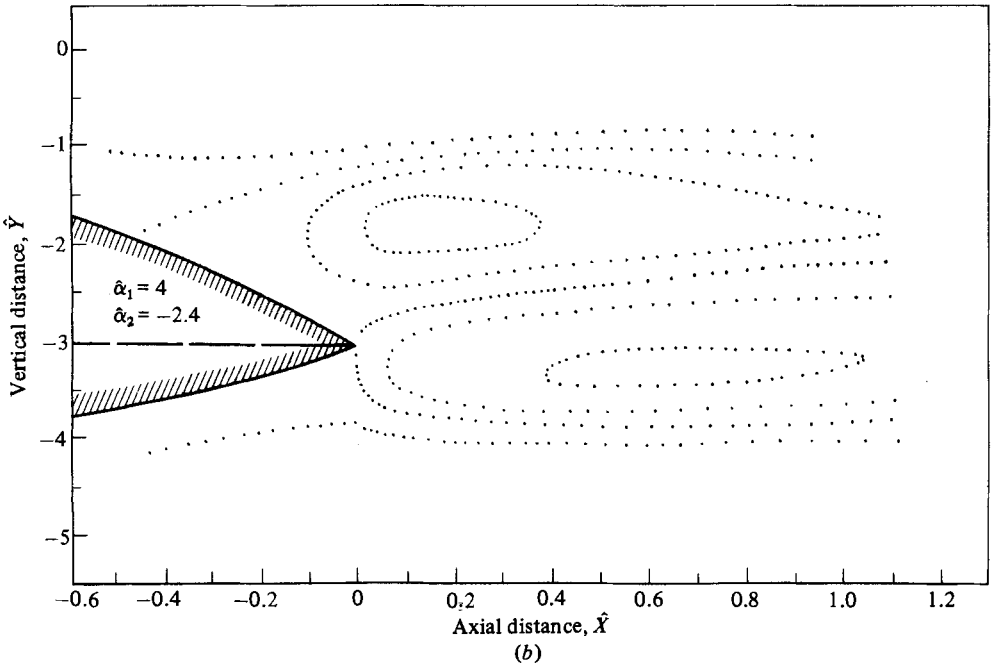

(*b*)

FIGURE 6(*a*, *b*). For caption see p. 237.

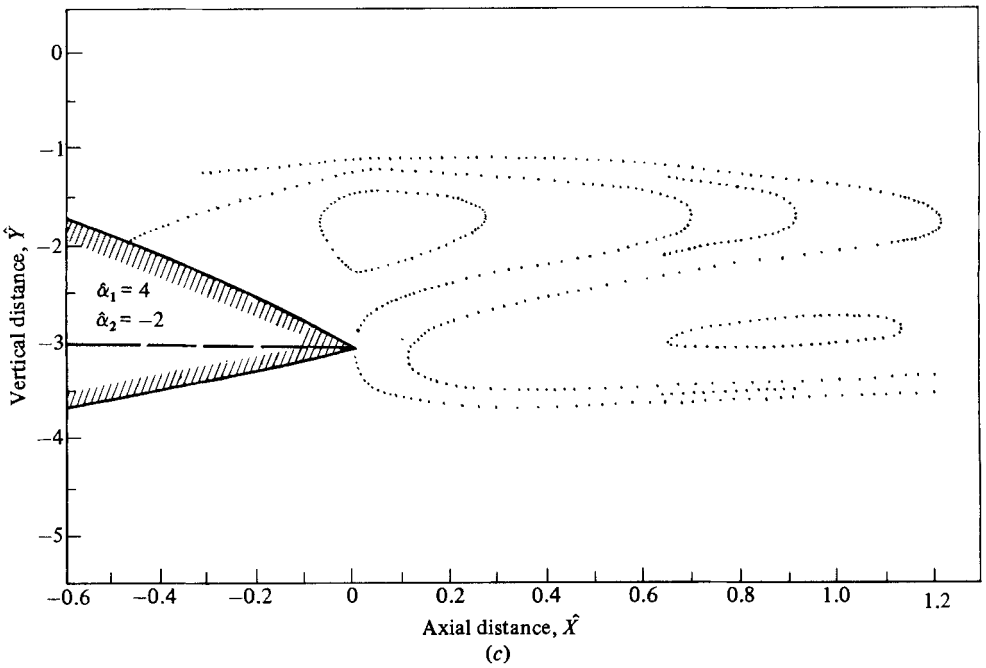

(*c*)

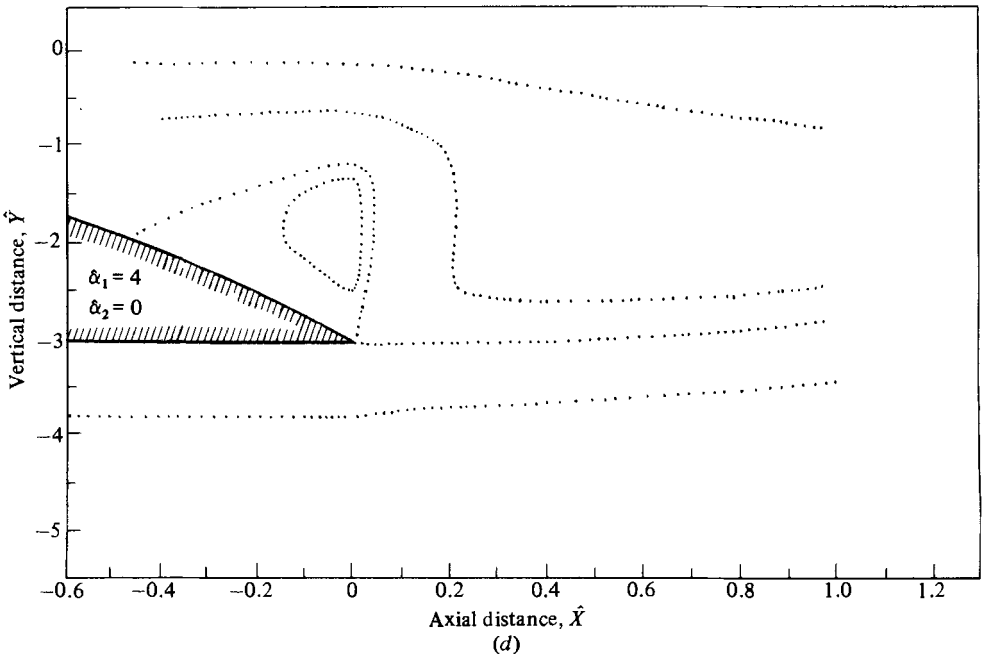

(*d*)

FIGURE 6(*c*, *d*). For caption see facing page.

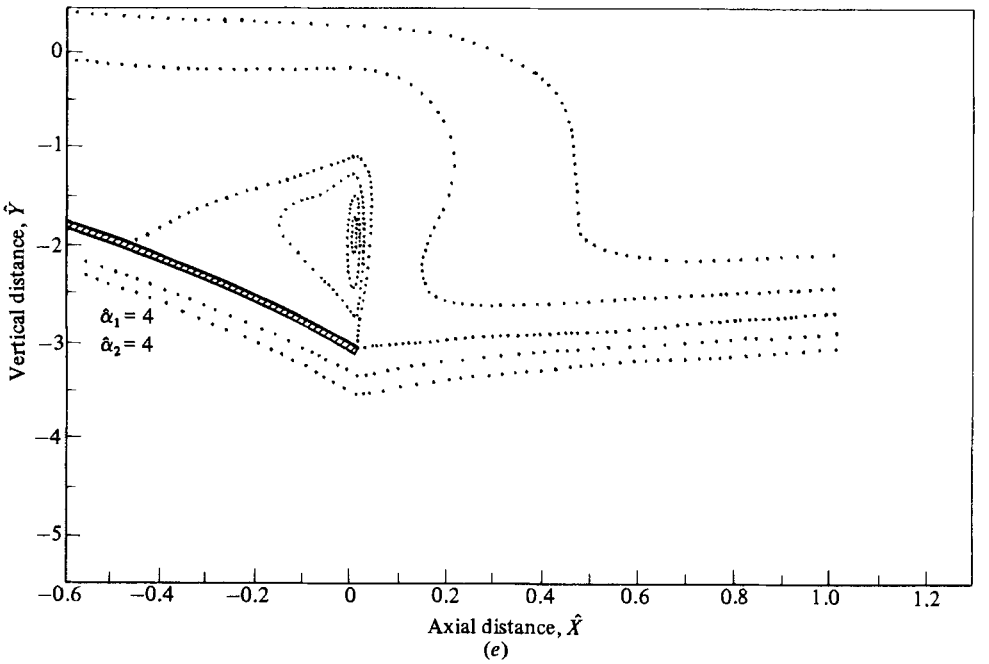

FIGURE 6. Streamlines for condensed trailing-edge flows with separation. (*a*) symmetric geometry, $\hat{\alpha}_2 = -4$; (*b*) slight non-symmetry, $\hat{\alpha}_2 = -2.4$; (*c*) moderate non-symmetry, $\hat{\alpha}_2 = -2$; (*d*) large non-symmetry, $\hat{\alpha}_2 = 0$; (*e*) complete non-symmetry, $\hat{\alpha}_2 = 4$. Throughout $\hat{\alpha}_1 = 4$.

where, from (2.5*a–c*), $G_0 = G$ for λ_+ zero. This gives forward flow with $G_0''(\infty) = 0$ but $G_0(\infty) = \lambda_-^{\frac{1}{3}} C_0$, where $C_0 = 1.2521$ from Stewartson & Williams (1973), implying that SP_1 entrains fluid from SP_2 (figure 7*a*). In SP_2 the fluid is slower moving, with

$$\Psi = \Delta^3 \tilde{\Psi}_2 + \ldots, \quad U = \Delta^2 \tilde{U}_2 + \ldots, \quad \overline{Y} = \Delta \tilde{Y}_2 > 0. \tag{4.5}$$

Here (2.2*a–g*) with (2.3) or (2.4) and the match with SP_1 imply the inviscid nonlinear governing equations

$$\tilde{U}_2 = \frac{\partial \tilde{\Psi}_2}{\partial \tilde{Y}_2}, \quad \tilde{U}_2 \frac{\partial \tilde{U}_2}{\partial \tilde{X}} - \frac{\partial \tilde{\Psi}_2}{\partial \tilde{X}} \frac{\partial \tilde{U}_2}{\partial \tilde{Y}_2} = -\frac{\mathrm{d}\tilde{P}}{\mathrm{d}\tilde{X}} \tag{4.6a}$$

and the boundary and starting conditions

$$\tilde{\Psi}_2 \to \lambda_-^{\frac{1}{3}} C_0 \tilde{X}^{\frac{2}{3}} \quad \text{as} \quad \tilde{Y}_2 \to 0+ \quad \text{(entrainment)}, \tag{4.6b}$$

$$\tilde{\Psi}_2 = \tfrac{1}{6}\mu \tilde{Y}_2^3 + \tfrac{1}{2}\tilde{\lambda}_+ \tilde{Y}_2^2, \quad \tilde{U}_2 = \tfrac{1}{2}\mu \tilde{Y}_2^2 + \tilde{\lambda}_+ \tilde{Y}_2 \quad \text{at} \quad \tilde{X} = 0+ \quad \text{(start)}, \tag{4.6c}$$

$$\tilde{\Psi} \sim \tfrac{1}{6}\mu \tilde{Y}_2^3 + \tfrac{1}{2}\tilde{\lambda}_+ \tilde{Y}_2^2 + o(1), \quad \tilde{U}_2 \sim \tfrac{1}{2}\mu \tilde{Y}_2^2 + \tilde{\lambda}_+ \tilde{Y}_2 + o(1) \quad \text{as} \quad \tilde{Y}_2 \to \infty$$
$$\text{(no displacement)}, \tag{4.6d}$$

where $\mu > 0$ is the adverse pressure gradient $\mathrm{d}P_+/\mathrm{d}X$ necessary at $X = 0-$ to drive the flow upstream of the trailing edge to the verge of separation (since $0 < \lambda_+ \ll 1$). Thus for λ_+ identically zero the profile at the trailing edge has the regular separation-point form $\Psi_+ \sim \frac{1}{6}\mu \overline{Y}^3$, $U_+ \sim \frac{1}{2}\mu \overline{Y}^2$ as $\overline{Y} \to 0+$. In (4.6*d*) the zero-displacement condition follows from reasoning virtually the same as that for (2.5*c*) and (2.8*e*), (2.9): a non-zero displacement (outside SP_2 of figure 7) would provoke too large a pressure response from (2.3) or (2.4) to be compatible with (4.1).

The solution for $\tilde{\Psi}_2$, $\tilde{U}_2$, $\tilde{P}$ in (4.6*a–d*) can be obtained using characteristics, for

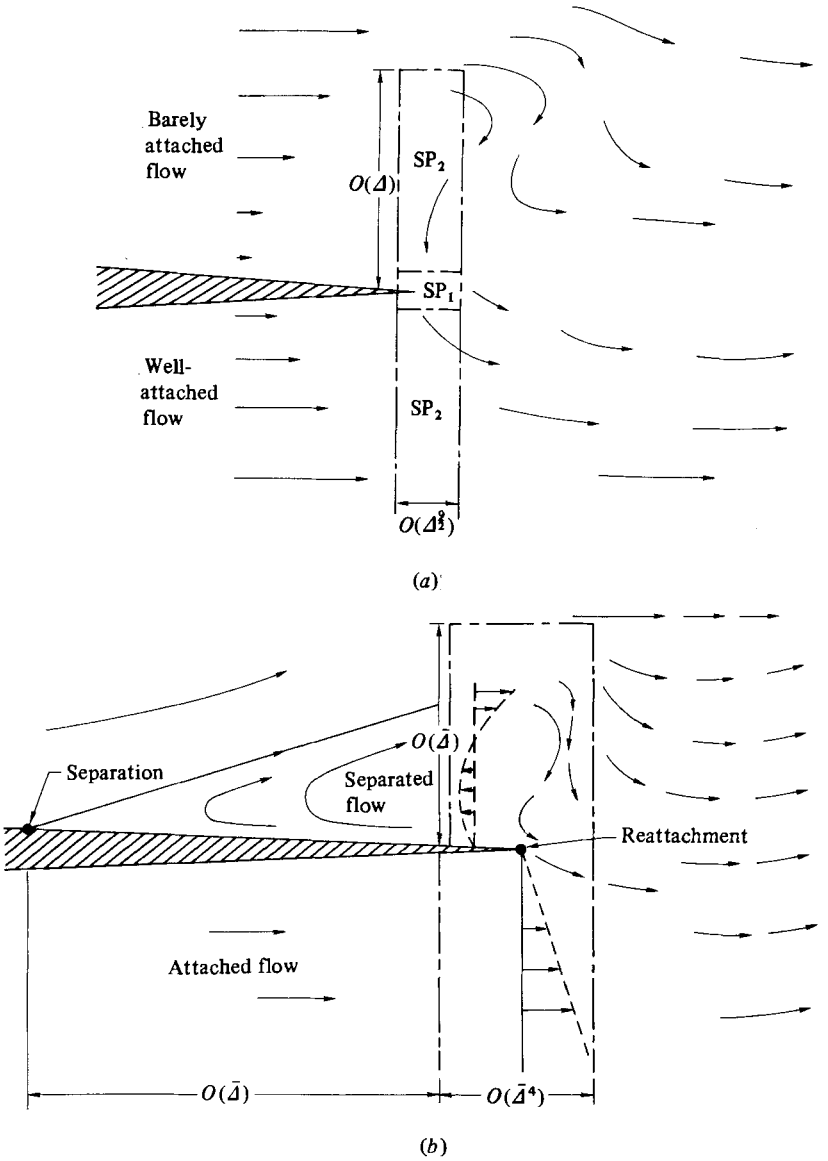

FIGURE 7. The limit flow structures near the separation angle $\alpha = \alpha_c$: (*a*) the pre-separated stage, $\alpha = \alpha_c -$ (see §4.2); (*b*) the post-separated stage, $\alpha = \alpha_c +$ (see §4.3).

example as in Cole & Aroesty (1968), but its principal features are deducible from its forms for small and large $\tilde{X}$. For small $\tilde{X}$ we find

$$\tilde{\Psi}_2(\tilde{X}, \tilde{Y}_2) = (\tfrac{1}{6}\mu\tilde{Y}_2^3 + \tfrac{1}{2}\tilde{\lambda}_+ \tilde{Y}_2^2) + \tilde{X}^{\frac{3}{2}}\tilde{P}_{\frac{3}{2}}\left[\frac{1}{\tilde{\lambda}_+} + \frac{\mu\tilde{Y}_2}{\tilde{\lambda}_+^2} + \mu\tilde{Y}_2\left(1 + \frac{\mu\tilde{Y}_2}{2\tilde{\lambda}_+}\right)\ln\left(\frac{\tilde{Y}_2}{\tilde{Y}_2 + 2\tilde{\lambda}_+/\mu}\right)\tilde{\lambda}_+^{-2}\right], \quad (4.7a)$$

$$\tilde{P}(\tilde{X}) = \tilde{P}(0) + \tilde{X}^{\frac{3}{2}}\tilde{P}_{\frac{3}{2}} + \ldots, \quad \tilde{P}_{\frac{3}{2}} = \tilde{\lambda}_+ \lambda_-^{\frac{1}{2}} C_0. \quad (4.7b)$$

The pressure rises relatively fast, the adverse pressure gradient being large, $O(\Delta^{-\frac{1}{2}})$, as fluid is entrained into SP_1. The bulk of the incoming nearly separated flow continues forward into SP_2 nevertheless. Then, downstream, as $\tilde{X} \to +\infty$, the shear

effect of $\tilde{\lambda}_+$ in (4.6*c*, *d*) diminishes and we have

$$\tilde{\Psi}_2(\tilde{X}, \tilde{Y}_2) = \tilde{X}^{\frac{2}{3}}\tilde{g}(\tilde{\eta}_2) + O(\tilde{X}^{\frac{1}{3}}), \quad \tilde{P}(\tilde{X}) \propto \tilde{X}^{\frac{2}{3}}, \tag{4.7c}$$

where $\tilde{\eta}_2 \equiv \tilde{Y}_2/\tilde{X}^{\frac{2}{3}}$, so that the layer SP_2 expands like $\tilde{X}^{\frac{2}{3}}$. The function $\tilde{g}(\tilde{\eta}_2)$ is calculated by Daniels (1974) and has the property that $g'(0+) < 0$. Hence the flow is reversed in SP_2 for a finite range of values of $\tilde{\eta}_2$ far downstream. A tongue of fluid, drawn back towards the trailing edge before being turned anticlockwise forward by SP_1, exists in SP_2 at a finite positive value of $\tilde{X}$, and its width then grows like $\tilde{X}^{\frac{2}{3}}$ downstream. It persists until the longer $O(1)$ scale in X when the widths $\Delta^{\frac{3}{2}}\tilde{X}^{\frac{1}{3}}$, $\Delta\tilde{X}^{\frac{2}{3}}$ of SP_1, SP_2 become comparable and $O(1)$ in terms of $\bar{Y}$.

This gives a natural development from pre- to post-separated motion. The tongue of turning fluid present downstream in the pre-separated situation above closely approaches the trailing edge with its forefront position $< \Delta^{\frac{9}{2}}$ (from further analysis of (4.6*a*)–(4.7*b*)) as $\Delta = \alpha_c - \alpha \to 0$. It actually attaches to the trailing edge in the special case of the above when $\alpha = \alpha_c$ as in Daniels (1974). Its next response when α is increased above α_c is to pass its forefront just upstream of the trailing edge on the upper surface, according to the following structural account.

4.3. *Post-separated flow*

Suppose now that $\alpha = \alpha_c + \bar{\Delta}$, where $\bar{\Delta}$ is small and positive. Therefore, other things being equal, the separation takes place at a small $O(\bar{\Delta})$ distance upstream of the trailing edge. So, if $\lambda_- > 0$ still, we have the conditions (2.5*e*) which must be reconciled with (2.5*d*). Again the close neighbourhood of the trailing edge is the crucial area, but the lengthscales involved upstream have to be quite distinct from those of the pre-separation state considered in §4.2. For although the logarithmic irregularities arising in (4.7*a*), with $-|\tilde{\lambda}_+|$ replacing $\tilde{\lambda}_+$, are smoothed out by viscous action, the implied negative value of the small shear as $\tilde{Y}_2 \to 0+$ is not removable and it forces an irrevocable singularity at higher order. Moreover the SP_1–SP_2 type of structure permits no upstream influence in $\tilde{X} < 0$. So another structure is set up.

It is assumed initially for the sake of argument, and as a guide, that $\lambda_- > 0$ is small and $O(\bar{\Delta})$ also, $\lambda_- = \bar{\Delta}\tilde{\lambda}_-$, say, the properties for λ_- of $O(1)$ being obtainable by taking $\tilde{\lambda}_-$ large subsequently: see the penultimate paragraph of this subsection. Then the major streamwise lengthscale turns out to be $O(\bar{\Delta}^4)$ (see figure 7*b*), longer than that of the pre-separated flow of §4.2, but still tiny. With $X = \bar{\Delta}^4\bar{X}$, then, we have

$$(\Psi, U, P) = [\bar{\Delta}^3\Psi(\bar{X}, Z), \bar{\Delta}^2\bar{U}(\bar{X}, Z), \bar{\Delta}^4\bar{P}(\bar{X})] + \ldots \tag{4.8}$$

in the viscous sublayers of thickness $O(\bar{\Delta})$ adjoining the surface, and downstream, where $\bar{Y} = \bar{\Delta}Z$. From (2.2*a*–*g*), (2.3) or (2.4) the boundary-layer equations hold in full,

$$\bar{U} = \frac{\partial\bar{\Psi}}{\partial Z}, \quad \bar{U}\frac{\partial\bar{U}}{\partial\bar{X}} - \frac{\partial\bar{\Psi}}{\partial\bar{X}}\frac{\partial\bar{U}}{\partial Z} = -\frac{\mathrm{d}\bar{P}}{\mathrm{d}\bar{X}} + \frac{\partial^2\bar{U}}{\partial Z^2}, \tag{4.9a}$$

and the constraints are

$$\bar{U} = \bar{\Psi} = 0 \quad \text{at} \quad Z = 0 \quad \text{in} \quad \bar{X} < 0, \tag{4.9b}$$

$$\bar{P}_+ = \bar{P}_-, \quad \bar{U} \quad \text{regular in} \quad Z \quad \text{for} \quad \bar{X} > 0, \tag{4.9c}$$

$$\bar{\Psi}_+ \sim \tfrac{1}{6}\mu_+ Z^3 - \tfrac{1}{2}kZ^2 + 0, \quad \bar{U}_+ \sim \tfrac{1}{2}\mu_+ Z^2 - kZ + 0 \quad \text{as} \quad Z \to \infty, \tag{4.9d}$$

$$\bar{U}_- \sim \tfrac{1}{2}\mu_- Z^2 - \tilde{\lambda}_- Z + 0 \quad \text{as} \quad Z \to -\infty, \tag{4.9e}$$

$$[\bar{\Psi}_+, \bar{U}_+, \bar{P}_+] \sim [\tfrac{1}{6}\mu_+ Z^3 - \tfrac{1}{2}kZ^2, \tfrac{1}{2}\mu_+ Z^2 - kZ, \mu_+ \bar{X}] \quad \text{as} \quad \bar{X} \to -\infty, \tag{4.9f}$$

$$\bar{\Psi}_- = \tfrac{1}{6}\mu_- Z^3 - \tfrac{1}{2}\tilde{\lambda}_- Z^2, \quad \bar{U}_- = \tfrac{1}{2}\mu_- Z^2 - \tilde{\lambda}_- Z, \quad \bar{P}_- = 0 \quad \text{at} \quad \bar{X} = 0-, \quad Z < 0. \tag{4.9g}$$

Here $\mu_\pm$ are the $O(1)$ adverse pressure gradients just upstream of the $\bar{\Delta}^4$ region, while $-k < 0$ is the upper-surface skin friction there, scaled by $\bar{\Delta}$. Between the present $O(\bar{\Delta}^4)$ region near the trailing edge and the separation at a larger distance $O(\bar{\Delta})$ upstream the flow suffers little upstream influence, and so the adverse pressure gradient μ_+ forces only a relatively slowly changing separated motion: hence the condition (4.9f) upstream. On the tiny $O(\bar{\Delta}^4)$ scale, however, a sudden change does take place locally, although it has little effect on the rest of the flowfield. The outer constraints (4.9d, e) follow from arguments similar to those used earlier regarding the necessity of zero displacement to leading order, since the typical slope of the present region is so large, $O(\bar{\Delta}^{-3})$. Finally the condition (4.9g) holds because to leading order the lower-surface flow remains unaffected by the upper-surface flow features up to the trailing edge.

It is believed that the inner problem (4.9a–g) contains the resolution of the dilemma between (2.5d, e), as well as explaining the sudden trends observed numerically in §3 and figures 4–6. For on the upper surface the problem (4.9a–g) admits an infinity of upstream eigensolutions, the unknown multiplying coefficients of which may adjust themselves to comply with virtually any desired downstream constraint, in this case the requirement (2.5d). The upstream behaviour here has the form

$$\bar{\Psi}_+ = (\tfrac{1}{6}\mu_+ Z^3 - \tfrac{1}{2}kZ^2) + \text{Real}\left\{\sum_{n=1}^{\infty} C_n \mathrm{e}^{\beta_n \bar{X}} \mathscr{F}_n(Z)\right\} + O(\exp^2), \tag{4.10a}$$

$$\bar{P}_+ = \mu_+ \bar{X} + \text{Real}\left\{\sum_{n=1}^{\infty} \frac{l_n C_n \mathrm{e}^{\beta_n \bar{X}}}{\beta_n}\right\} + O(\exp^2) \tag{4.10b}$$

for $\bar{X} \to -\infty$, where $\exp^2$ indicates all the nonlinear inertial effects, and C_n, l_n are constants. When normalized, the eigenfunctions $\mathscr{F}_n(Z)$ and ordered eigenvalues β_n, which must have positive real parts, satisfy the linear equation and boundary conditions

$$\mathscr{F}'''_n - \tfrac{1}{2}\beta_n Z(Z-2)\mathscr{F}'_n + \beta_n(Z-1)\mathscr{F}_n = l_n, \tag{4.11a}$$

$$\mathscr{F}_n(0) = \mathscr{F}'_n(0) = \mathscr{F}_n(\infty) = 0, \tag{4.11b}$$

from (4.9a, b, d). The eigenvalue problem (4.11a, b) can be shown to govern also the first appearance of upstream influence in the boundary-layer equations just beyond a regular interactive separation in general. It is different from Stewartson's (1958) for classical separation, where, with prescribed pressure gradients, $l_n = 0$ and the condition on $\mathscr{F}_n^{(\infty)}$ in (4.11b) is relaxed to one requiring no exponential growth for large Z. Stewartson analysed the equation for large β_n but it is analysable also for any value of β_n, in terms of the coordinate $(Z-1)^2$, and a recent investigation suggests that the eigenvalue β_1 with smallest real part, dominating the upstream influence, is large (≈ 50 numerically – Smith 1983a). The number of eigenvalues is infinite, however, akin to those in classical boundary layers, for which

$$\beta_n \sim 8(N+\tfrac{1}{3})^2 \quad \text{for large integral } N. \tag{4.11c}$$

The multiplying coefficients C_n, $n \geqslant 1$, in (4.10a, b) remain undetermined as yet. Their values depend on, and influence, the entire flow solution for $O(1)$ values of $\bar{X}$ and are such that (2.5d) is satisfied, with the skin friction $\bar{\tau}_+ \equiv \partial \bar{U}_+ / \partial Z(\bar{X}, 0+)$ rising from $-k$ far upstream to a positive value at $\bar{X} = 0-$, according to the present description.

The necessary numerical treatment of (4.9a–g) was conducted with the sweeping scheme of §3. Without loss of generality, one may set $k = \mu_+ = 1$ henceforth with

$\tilde{\lambda}_- > 0$ and $\mu_- \geqslant 0$ then varying. Then take $\mu_- = 0$ as an example, for reasons given below, so that the lower-surface flow gives the uniform forward shear $\bar{U} = \tilde{\lambda}_- |Z|$ at $\bar{X} = 0-$. The solutions of (4.9*a–g*) in that case, with $\tilde{\lambda}_- = 1, 12$, are shown in figure 8(*a*, *b*). The upper-surface skin friction (figure 8*b*) rises from -1 to a positive value at $\bar{X} = 0-$, yielding the reattachment in $X < 0$ after the separation infinitely far upstream in $\bar{X}$. The pressure gradient (figure 8*a*) in turn changes from adverse upstream to favourable, as the small tongue of turning fluid is forced just upstream of the trailing edge. The phenomenon is strictly smooth in the $(\bar{X}, Z)$-frame, although an added complication is the largeness of β_1, which reduces the upstream influence substantially, and numerically required the use of fine grid spacing in the $\bar{X}$-direction again. The associated streamline pattern closely resembles that near the trailing edge in all of figures 6(*c–e*) but with stretching in the streamwise direction, similar to figure 7(*b*).

Far downstream the flow is completely forward, with

$$\left.\begin{aligned} &\bar{\Psi} \sim \bar{X}^{\frac{3}{4}} \bar{F}(\bar{\eta}) + O(\bar{X}^{\frac{1}{2}}), \\ &\bar{P}'(\bar{X}) \to 0 \end{aligned}\right\} \quad \text{as} \quad \bar{X} \to \infty, \tag{4.12}$$

predominantly. Here $\bar{\eta} = Z/\bar{X}^{\frac{1}{4}}$, and (4.9*a*) gives the similarity equation

$$\bar{F}''' + \tfrac{3}{4}\bar{F}\bar{F}'' - \tfrac{1}{2}\bar{F}'^2 = 0 \tag{4.13a}$$

for $\bar{F}(\bar{\eta})$, with the boundary conditions being

$$\bar{F} \sim \tfrac{1}{6}\bar{\eta}^3 + 0 \quad \text{as} \quad \bar{\eta} \to \infty, \quad \bar{F}'(-\infty) = 0 \tag{4.13b}$$

from (4.9*c–e*), for the case $\mu_- = 0$. The solution of (4.13*a*, *b*) gives $\bar{F}(-\infty) = -\bar{C}_0 (= -1.39)$ from Smith & Daniels (1981). Hence the pressure must increase again far downstream, with

$$\left.\begin{aligned} &\bar{\Psi} \sim -\tfrac{1}{2}\tilde{\lambda}_- Z^2 - \frac{\bar{P}(\bar{X})}{\tilde{\lambda}} \quad \text{as} \quad Z \to -\infty, \\ &\bar{P} \sim \tilde{\lambda}_- \bar{C}_0 \bar{X}^{\frac{3}{4}} \quad \text{as} \quad \bar{X} \to \infty, \end{aligned}\right\} \tag{4.13c}$$

from the extension $\bar{\Psi} \sim -\frac{1}{2}\tilde{\lambda}_- Z^2 - \bar{P}(\bar{X})/\tilde{\lambda}_-$ $(Z \to -\infty)$ of the lower condition (4.9*e*) for $\mu_- = 0$. With $\mu_- = 0$ there is also an outer domain far downstream, of thickness $O(\bar{X}^{\frac{3}{8}})$, below the $O(\bar{X}^{\frac{1}{4}})$ domain of (4.12), therefore. The trend (4.13*c*) is fairly in line with that of the numerical results in figure 8. Further, the behaviour (4.12), (4.13*a–c*) indicates that the present region of thickness $O(\bar{\Delta})$ grows to $O(1)$ thickness beyond the trailing edge as X becomes $O(1)$ again $(\bar{X} \to O(\bar{\Delta}^{-4}))$, with forward flow there; while to leading order the small shears $\bar{\Delta}\bar{\tau}$ $(= \tau)$ on the lower surface and $-\bar{\Delta}k$ on the upper have negligible global effect. This too ties in with the earlier numerical results of §3, especially with regard to the dramatic flow features of figure 6 when λ_- is small but positive.

The above holds when $\lambda_- > 0$ is small, but the flow properties when $\lambda_- > 0$ is $O(1)$ emerge next, simply by taking $\tilde{\lambda}_-$ to be large. Then the limit problem develops as follows. When $\bar{X}$ is large, positive and $O(\tilde{\lambda}_-^4)$ the major scale in Z is of order $\tilde{\lambda}_-$, while $\bar{\Psi}$, $\bar{U}$, $\bar{P}$ have the orders $\tilde{\lambda}_-^3$, $\tilde{\lambda}_-^2$, $\tilde{\lambda}_-^4$, respectively. So the boundary-layer equations hold in full, subject to the separation form $\bar{\Psi} \sim Z^3$ at the upper extremity in Z and to the forward shear $\bar{\Psi} \sim |Z|$ at the lower. For smaller $\bar{X}$ the lower shear force dominates, giving mainly a strong suction effect on the upper-surface flow and forcing the necessary reattachment there. The influence of μ_- is then negligible, as in the

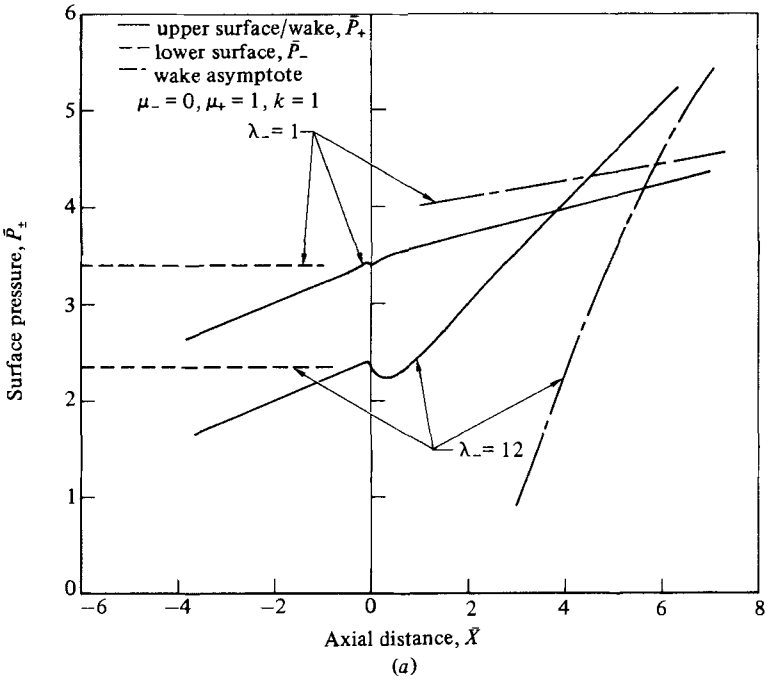

FIGURE 8(a). For caption see facing page.

calculations above. For $\bar{X}$ of order $\tilde{\lambda}_-^4$, however, the extreme upper forward flow reasserts itself and gradually drags the upper part of the motion forward again. Finally, for $\bar{X}$ greater than that, the conditions (4.12)–(4.13c) are achieved. Therefore the characteristic adjustment length from reversed to forward flow downstream of the trailing edge is increased to $O(\tilde{\lambda}_-^4)$ in terms of $\bar{X}$, i.e. to $O(\tilde{\lambda}_-^4\,\bar{\Delta}^4)$ in terms of the original coordinate X.

Converting that to the flow structure holding for λ_- actually $O(1)$ (i.e. taking $\tilde{\lambda}_-$ to be $O(\bar{\Delta}^{-1})$) we have the result that the main length of the reversed-flow zone downstream of the trailing edge must be $O(1)$ in X then, whereas upstream the initial influence of the reattachment process adheres to the tiny $\bar{\Delta}^4$ scaling in X. In addition, a smaller $\frac{9}{2}$ streamwise lengthscaling like that in §4.2, i.e. $X = O(\bar{\Delta}^{\frac{9}{2}})$ here, comes back into operation when λ_- is $O(1)$, but the initial profile involved does not have the simple form (4.6c). Instead, reversed flow is present through interaction between the $\bar{\Delta}^4$ scale further upstream ($\bar{X} \to 0-$) and the more local $\bar{\Delta}^{\frac{9}{2}}$ scale (as $\bar{\Delta}^{-\frac{9}{2}}X \to -\infty$), and reattachment must ensue ahead of $\Delta^{-\frac{9}{2}}X = 0$ by means of (4.6a).

The upshot of this structural view of post-separated flows is the prediction that, first, a tiny lengthscale $O(\bar{\Delta}^4)$ comes into play around the trailing edge when the typical negative minimum of the skin friction on the surface with separation is small, of order $-\bar{\Delta}$; secondly, reattachment takes place within that lengthscale, or a shorter one, in contrast with the much larger upstream separation distance, and it resolves the difficulty over (2.5d, e); and, thirdly, the global effect of this last, sudden but tiny-scaled, adjustment is small. These aspects appear to be reflected well in the post-separation results of §3, and would seem to account for the numerical difficulties which had to be addressed there. In particular, since $\bar{\Delta}$, measured in terms of $-\tau_+$ in figures 4 and 5, is typically 0.1, the implied $O(\bar{\Delta}^4)$ streamwise lengthscale is of the order of 10^{-4} near the trailing edge.

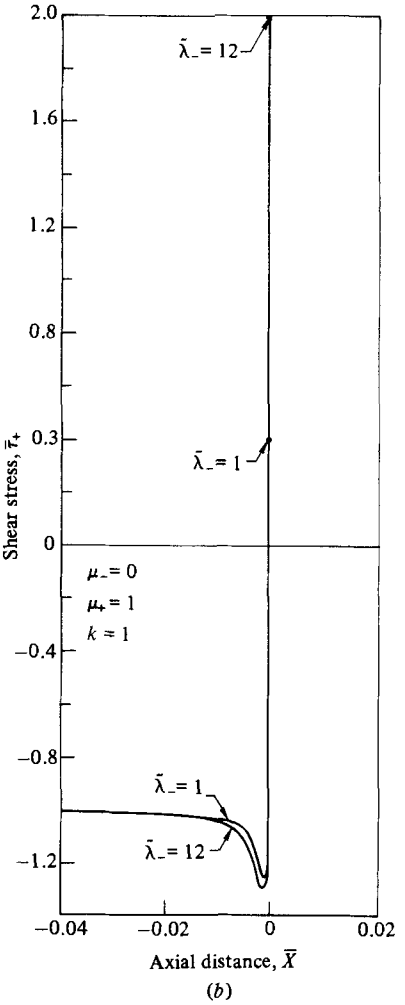

FIGURE 8. Post-separated limit solutions (see §4.3) for (*a*) the pressure; (*b*) the surface shear stress.

5. Concluding remarks

One of the principal aims of this study has been to investigate non-symmetric trailing-edge flows with one-sided separation, where (2.5*e*) holds, and their relation to the condition (2.5*d*) requiring forward flow at the onset of the trailing edge. There is no doubt that the presence of one-sided separation itself provides the very mechanism for the satisfaction of (2.5*d*) by permitting upstream influence through the reversed flow. So certainly (2.5*e*) does not necessarily contradict (2.5*d*). The evidence from our numerical work of §3 coupled with the structural forms of pre- and post-separated flows put forward in §4 is quite strongly that the above mechanism does indeed act to make the one-sided separating flow consistent with (2.5*d*). A tongue of anticlockwise turning fluid is drawn just ahead of the trailing edge to yield a *reattachment* of the local upper-surface flow, with forward flow then proceeding to the trailing edge exactly as required by (2.5*d*).

This phenomenon can force a rather dramatic response in the overall flowfield, as

figure 6 shows, but nevertheless it appears to be not unreasonable physically,† especially when set against the properties of pre-separated motion or of two-sided separating flows. In the former case the tongue of turning fluid already exists, beyond the trailing edge, when the upper-surface flow is just attached. Then, on the verge of upper-surface separation, the tongue moves upstream to virtually touch the trailing edge, apparently presaging the further movement upstream required in the post-separated state. Similarly, in two-sided separating flow the two symmetric eddies present for a thick symmetric trailing edge are gradually distorted and turned as non-symmetry is introduced, say by making the lower-surface flow gradually stronger. The downstream end of the upper eddy is pushed upstream, the lower eddy decreases in size and is pushed further downstream, and upper-surface fluid pours round and between them, encircling the lower eddy in particular before passing to downstream infinity. This creates the tongue of anticlockwise-turning fluid close to the trailing edge in readiness for the crossover to one-sided separation (as α_2 passes through the value α_c in §3). There the lower eddy seems to disappear eventually, but the tongue remains and is intensified by the effective suction of the stronger flow leaving the lower surface, and therefore the upper eddy is forced to close more abruptly.

The abruptness of the upper eddy closure then, and of the allied reattachment of the tongue on to the upper surface, fall in well with the analytically based account of the post-separated regime in §4.3. According to §4.3, a tiny pressure fall acts abruptly, over a tiny distance, to produce a sizeable favourable pressure gradient which forces the reattachment. The typical length involved in the closure of the upper eddy and the intensity of the upstream-facing tongue rapidly decrease and increase respectively as the lower surface skin friction becomes more positive. Upstream, however, the small lengthscale controlling the overall adjustment of the upper-surface flow from a separated state to a reattached state close to the surface is generally of order $(-\tau_+^{\min})^4$. This is tiny, even compared with the theoretically small upstream separation distance $O(-\tau_+^{\min})$. Subsection 4.3 seems to provide firm structural support for the rapidity of the reattachment process observed numerically then, as well as for the subsequent sudden plunge of the upper-surface fluid towards the lower (due to entrainment) followed by the more gradual recovery of forward motion as the upper flow speed increases again, with a rising pressure.

Given such tiny lengthscales and sudden adjustments of the flowfield, it is not so surprising that the calculation of one-sided separating flows is initially at its most sensitive near the trailing edge. Yet both the numerical scheme of §3 and a quite different one developed by Dr M. J. Werle (see also Elliott & Smith 1983; Burggraf 1983) give exactly the same strong trends towards upper-surface reattachment as they converge, including the effects of grid refinement, and they both seem to reflect reasonably well the short lengthscales involved. Essential to the numerical treatment here is the use of windward differencing to accommodate the reversed-flow influence (this influence is the one major factor controlling the flow response in the post-separated regime) and the acknowledgement of the discontinuities across the trailing-edge

† Dr M. J. Werle has kindly pointed out Hegna's (1981, e.g. his figures 3, 13, 14) recent numerical solutions of the Navier–Stokes equations for non-symmetric trailing-edge flows, with turbulence modelling, and the turbulent/laminar flow calculations and/or experiments of Solignac (1980, see his figures 2*a*, *b*, 6–8), Viswanath & Brown (1982), Le Balleur (1981, e.g. his figures 9, 19, 20, 30). See also Mehta & Lavan (1975) and Mehta (1977). All of these works, for laminar or even turbulent flow, appear to fall well in line with the present account, in terms of their streamlines, vorticity fields or velocity profiles, and this is an encouraging feature.

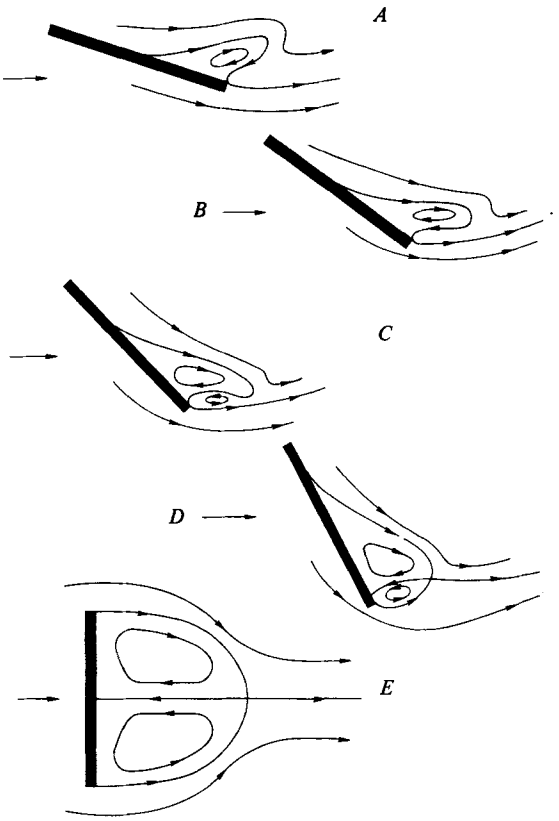

FIGURE 9. Possible development of the flow past a thin airfoil as the angle of incidence is increased (not to scale). An alternative, however, is the development of a single predominant eddy. See also §5, and, on the unsteady evolution, Mehta & Lavan (1975), Mehta (1977) and Smith (1982*b*).

station. Away from the trailing edge the flow calculation is much less sensitive, which is an encouraging feature, and the flow features that emerge (above) are virtually independent of the differencing techniques adopted right at the trailing edge and of the change in the solution very close to the trailing edge before convergence is attained. Once again, therefore, there is a tie-in to the structural description of §4.3.

The above supports the view that one-sided separation ahead of the trailing edge is a continuous and natural development from attached flow or from double-sided separation as the parameter α, say, governing the non-symmetry is increased. There is no catastrophic stall. It is avoided by the reattachment, ahead of the trailing edge, of the tongue of turning fluid. Any irregularities involved as α passes through the incipient separation value α_c are relatively weak, therefore, confined to higher derivatives with respect to α, as regards the overall properties of the motion such as downwash, circulation, lift and drag. These conclusions apply to both the condensed-flow and the triple-deck descriptions.

At this stage it is interesting to speculate on the subsequent behaviour of the flowfield as α is increased still further. Initially we expected two recirculating eddies to be present in the immediately post-separated regime anyway, but the results above indicate that this need not be so. The upstream reattaching tongue of turning fluid can be supplied from downstream either by the plunge of upper-surface fluid or by the upstream end of a second, lower, anticlockwise-rotating eddy. The former

happens, apparently, for the thin drooped trailing edge. Further increase of the non-symmetry may reinstate the second eddy, however, as the accelerated flow off the lower surface and the plunging section of upper-surface fluid are then forced closer together. Ultimately a smooth connection (rather than the discontinuous one suggested in previous works) is possible, in principle, with the grossly separated flow structure expected for trailing edges with asymptotically larger non-symmetry, e.g. at increased angle of attack. The upper-surface separation point is pushed far upstream, the reattachment point also, possibly, and the wake effect is much enhanced with perhaps two or more elongated eddies present. For the condensed problem the connection then is made with a structure like that of Smith & Daniels (1981). A distinct separated shear layer rides high over the trailing edge, entraining fluid from below, while the lower-surface flow sets up another strong shear layer beyond the trailing edge. The necessary supply of entrained fluid is provided exactly by the viscous coalescence of the two shear layers far downstream, and solutions for the entraining motion are found to allow the required reattachment to occur, on the upper surface ahead of the trailing edge, in a relatively gentle fashion. For the triple-deck problem the connection can readily be made to an upstream separation of the Sychev (1972) – Messiter (1975) – Smith (1977) form in subsonic flow, and of the Stewartson & Williams (1973) – Neiland (1971) form in supersonic flow, in principle. The flow structure then has some broad resemblance to that for the condensed problem, although by contrast its complete features have still to be delineated. Here, incidentally, there is no significance in the closeness of the reduced angles 0.47, 2.050 for subsonic or supersonic incipient separation in the non-aligned flat-plate studies noted earlier for the triple-deck problem and the sometimes-associated values 0.44, 1.800 of Smith (1977), Williams (1975) (cf. the respective values 0.42+, 1.790 of Korolev 1980*a*; Curle 1982) controlling upstream breakaway separation. The latter values come into play only through the smooth limiting connection ($\alpha \to \infty$) described above, we believe. After that a still further increase of the non-symmetry beyond the triple-deck scale can be expected to disturb the global flowfield significantly, compared with the mainly local effects produced before. There is an interesting adjustment possible now, from the small, nonsymmetric, double eddy structure† to the large double-eddy structure of grossly separated flow as, say, we gradually turn a flat plate until it is normal to the outer free stream (see figure 9). The same end result can be obtained, in principle, by thickening the symmetric trailing-edge geometry of figure 6 (*a*) and/or compressing the associated airfoil length, as in Cheng & Smith (1981), rather than going through the non-symmetric process of figures 6 (*a*)–(*e*). There is also the prospect that the gradually increasing eddies near the trailing edge may so disturb the global flowfield that eventually a castrophic leading-edge stall of the theoretical (Stewartson, Smith & Kaups 1982; Smith 1982*b*) kind is provoked on a round-nosed airfoil subjected to increased non-symmetry. The last-named paper emphasizes the increased role of unsteadiness in such an event.

† The flow structure may well be non-unique, of course, but that remains to be seen (see also Smith 1983*b*). If, for instance, there is a single dominant eddy present near the trailing edge, accompanied by the subsequent plunge and reverse of the tongue of turning fluid (as in figures 6*c*–*e*), with or without a weaker eddy downstream, this may be the embryonic version of the highly nonsymmetric flowfields often observed in practice for bluff body motions. See Batchelor's (1967) plates 2, 4, 7, 10, 11, for example. Again it would be of great interest to follow the unsteady development of the flowfields without, but more especially with, non-symmetry present.

I am indebted to Dr M. J. Werle, whose great help, advice, encouragement and enthusiasm throughout this work were vital. He and Drs J. E. Carter, V. N. Vatsa and J. M. Verdon are thanked for their sustained interest and comments. The bulk of the work was carried out during a visit to the United Technologies Research Center, East Hartford, Connecticut, U.S.A., in July–September 1981 and was partially supported through Dr. R. E. Whitehead of the Office of Naval Research, U.S.A., under Contract N00014-81-C-0381. Subsequent computer support from the SERC, U.K., is also acknowledged.

Appendix. If two-sided separation is present

When the triple-deck or condensed flow on both the upper and lower surfaces is separated at the trailing edge, then the velocity profile $U = U_0(\bar{Y}) = \Psi_0'(\bar{Y})$ in the near-wake ($X = 0+$) is non-zero and negative at $\bar{Y} = 0$. Hence the irregularity across the trailing-edge station is concentrated mostly on the upstream side $X < 0$, $|X| \ll 1$, where it has a Blasius-like form involving a $|X|^{\frac{1}{2}}$ dependence rather than the more usual $X^{\frac{1}{3}}$ dependence encountered in Goldstein-like wakes.

For X small and negative we have

$$\Psi = |X|^{\frac{1}{2}} f_B(\eta) + \ldots, \quad \eta = \frac{\bar{Y}}{|X|^{\frac{1}{2}}}, \tag{A 1}$$

where f_B satisfies the Blasius equation

$$\left.\begin{aligned} 2f'''_B - f_B f''_B = 0 \quad \text{with} \quad f_B(0) = f'_B(0) = 0, \\ f'_B(\infty) = -U_0(0) < 0 \end{aligned}\right\} \tag{A 2}$$

from (2.2*a–c*), provided that P is finite at $X = 0$ (see (A 4)). Hence $\Psi \sim U_0(0)(\bar{Y} - \Delta_{\pm}^{(1)}|X|^{\frac{1}{2}})$ at the edge of the thin Blasius-type layer, where the known constant $\Delta_{\pm}^{(1)}$ represents the effective Blasius displacement. Further out, for $\bar{Y}$ of order unity, the solution therefore expands in the form

$$\Psi_{\pm} = \Psi_0(\bar{Y}) + |X|^{\frac{1}{2}} \Psi_{\pm}^{(1)}(\bar{Y}) + \ldots, \tag{A 3}$$

while

$$P_{\pm}(X) = P(0) + |X|^{\frac{1}{2}} P_{\pm}^{(\frac{1}{2})} + \ldots. \tag{A 4}$$

From (2.2*a*, *b*) we obtain

$$\Psi_{\pm}^{(1)} = -U_0(\bar{Y}) \left[\Delta_{\pm}^{(1)} + P_{\pm}^{(\frac{1}{2})} \int_0^{\bar{Y}} \frac{\mathrm{d}\bar{Y}}{(U_0(\bar{Y}))^2} \right], \tag{A 5}$$

after matching with the Blasius-type layer as $\bar{Y} \to 0$. Then the match with the outer displacement constraint (2.2*e*) requires that

$$P_{\pm}^{(\frac{1}{2})} = -\frac{\Delta_{\pm}^{(1)} + q^{\pm}}{\int_0^{\pm\infty} (U_0(\bar{Y}))^{-2} \, \mathrm{d}\bar{Y}}, \tag{A 6}$$

where $F_{\pm}(X) \sim q^{\pm}|X|^{\frac{1}{2}}$ as $X \to 0-$, so that the trailing edge can be blunt. The pressure–displacement relation (2.3) or (2.4) has also been used in conjunction with (A 5) to give the result (A 6) for the local pressure.

We note that the principal value of the integral in (A 5) is required for the jump across the irregularity at the critical level $\bar{Y} = \bar{Y}_c$, where $U_0(\bar{Y}_c) = 0$. It can be shown

that the irregularity here is smoothed out mainly in a thin layer of thickness $O(|X|^{\frac{1}{4}})$ centred at $Y = Y_c$.

REFERENCES

BATCHELOR, G. K. 1967 *An Introduction to Fluid Dynamics*. Cambridge University Press.

BROWN, S. N. & CHENG, H. K. 1981 *J. Fluid Mech.* **108**, 171.

BROWN, S. N. & STEWARTSON, K. 1970 *J. Fluid Mech.* **42**, 561.

BURGGRAF, O. R. 1983 In preparation.

CARTER, J. E. 1974 *AIAA paper* 74–583.

CARTER, J. E. 1979 *AIAA paper* 79–1450.

CARTER, J. E. & WORNOM, S. F. 1975 *NASA* SP-347, 125.

CHENG, H. K. & SMITH, F. T. 1982 *Z. angew. Math. Phys.* **33**, 151.

CHOW, R. & MELNIK, R. E. 1976 *Grumman Res. Dept. Rep.* RE-526J. [Also in *Proc. 5th Intl Conf. Num. Methods in Fluid Dyn.* (ed. A. I. van de Voore & P. J. Zauberger). Lecture Notes in Physics, vol. 59, p. 135.]

COLE, J. D. & AROESTY, J. 1968 *Int. J. Heat Mass Transfer* **11**, 1167.

CURLE, N. 1982 *Proc. R. Soc. Lond.* **A379**, 217.

DANIELS, P. G. 1974 *J. Fluid Mech.* **63**, 641.

ELLIOTT, J. W. & SMITH, F. T. 1983 In preparation.

HAKKINEN, R. J. & ROTT, N. 1965 *AIAA J.* **3**,

HEGNA, H. A. 1981 *AIAA paper* 81-0047, *presented at AIAA 19th Aerospace Sci. Mtg*, 12–15 *Jan.* 1981, *St Louis, Missouri, U.S.A.* [Also: The numerical solution of incompressible turbulent flow over airfoils. Ph.D. Thesis.]

JOBE, C. E. & BURGGRAF, O. R. 1974 *Proc. R. Soc. Lond.* **A340**, 91.

KOROLEV, G. L. 1980*a* *Sci. J. TSAGI* **11**(2), 27.

KOROLEV, G. L. 1980*b* *Sci. J. TSAGI* **11**(4), 8.

LE BALLEUR, J-C. 1981 *Rech. Aérospatiale* **3**, 21.

MEHTA, U. B. 1977 In *Unsteady Aerodynamics, AGARD Conf. Proc.* CP-227, *paper* 23.

MEHTA, U. B. & LAVAN, Z. 1975 *J. Fluid Mech.* **67**, 227.

MELNIK, R. E. & CHOW, R. 1975 *Grumman Res. Dep. Rep.* RE-510. [Also in *Proc. NASA Conf. Aerodyn. Analysis Requiring Advanced Computations*, 1975.]

MESSITER, A. F. 1970 *SIAM J. Appl. Maths* **18**, 241.

MESSITER, A. F. 1975 *AGARD Conf. Proc., paper* 168 on flow separation.

MESSITER, A. F. 1979 In *Proc. 8th U.S. Natl Appl. Maths Congr., Los Angeles*, 1978.

NEILAND, V. YA. 1971 *Izv. Akad. Nauk SSSR, Mekh. Zhid i Gaza* No. 3.

REYHNER, T. A. & FLÜGGE-LOTZ, I. 1968 *Int. J. Nonlinear Mech.* **3**, 173.

RUBAN, A. I. & SYCHEV, V. V. 1979 *Adv. Mech.* **2**, 57.

SMITH, F. T. 1976 *Q. J. Mech. Appl. Maths* **29**, 343; **29**, 365.

SMITH, F. T. 1977 *Proc. R. Soc. Lond.* **A356**, 433.

SMITH, F. T. 1982*a* *Review, IMA J. Appl. Maths* **28**, 207.

SMITH, F. T. 1982*b* *Aero. Q.* Nov. 1982, 331.

SMITH, F. T. 1983*a* Submitted to *Q. J. Mech. Appl. Maths.*

SMITH, F. T. 1983*b* Submitted to *Proc. R. Soc. Lond.* **A**.

SMITH, F. T., BRIGHTON, P. W. M., JACKSON, P. S. & HUNT, J. C. R. 1981 *J. Fluid Mech.* **113**, 123.

SMITH, F. T. & DANIELS, P. G. 1981 *J. Fluid Mech.* **110**, 1.

SMITH, F. T. & MERKIN, J. H. 1982 *Comp. & Fluids* **10**, 7.

SOLIGNAC, J-L. 1980 *Rech. Aérospatiale* **3**, 65.

STEWARTSON, K. 1958 *Q. J. Mech. Appl. Maths* **11**, 398.

STEWARTSON, K. 1969 *Mathematika* **16**, 106.

STEWARTSON, K. 1974 *Adv. Appl. Mech.* **14**, 145.

STEWARTSON, K. 1981 *SIAM Rev.* **23**, 308.

STEWARTSON, K., SMITH, F. T. & KAUPS, K. 1982 *Stud. Appl. Maths* **67**, 45.

STEWARTSON, K. & WILLIAMS, P. G. 1973 *Mathematika* **20**, 98.

SYCHEV, V. V. 1972 *Izv. Akad. Nauk SSSR, Mekh. Zhid i Gaza* **3**, 47.

VATSA, V. N., WERLE, M. J. & VERDON, J. M. 1981 *United Technologies Res. Center Rep.* R81-914986-5; or *AIAA paper* 82-0165, *presented at AIAA 20th Aerospace Sci. Meeting, Jan.* 1982, *Orlando, Florida.*

VELDMAN, A. E. P. 1980 *Netherlands Natl Aerospace Lab. Rep.* NLR TR 79023.

VELDMAN, A. E. P. & DIJKSTRA, D. 1981 In *Proc. 7th Intl Conf. Num. Methods in Fluid Dyn.* (ed. W. C. Reynolds & R. W. MacCormack). Lecture Notes in Physics, vol. 141. Springer.

VELDMAN, A. E. P. & VOOREN, A. I. VAN DE 1975 In *Proc. 4th Intl Conf. Num. Methods in Fluid Dyn.* (ed. R. D. Richtmyer). Lecture Notes in Physics, vol. 35, p. 422. Springer.

VISWANATH, P. R. & BROWN, J. L. 1982 *AIAA paper* 82–0348, *presented at AIAA 20th Aerospace Sci. Meeting, Jan.* 1982, *Orlando, Florida.*

WERLE, M. J. & VERDON, J. M. 1980 In *Proc. Int. Conf. Boundary and Interior Layers, June* 1980, *Trinity College, Dublin.*

WILLIAMS, P. G., 1975 In *Proc. 4th Int. Conf. Num. Methods in Fluid Dyn.* (ed. R. D. Richtmyer). Lecture Notes in Physics, vol. 35. Springer.